

CORRELATIONS IN QE(LIKE) NEUTRINO- NUCLEUS SCATTERING

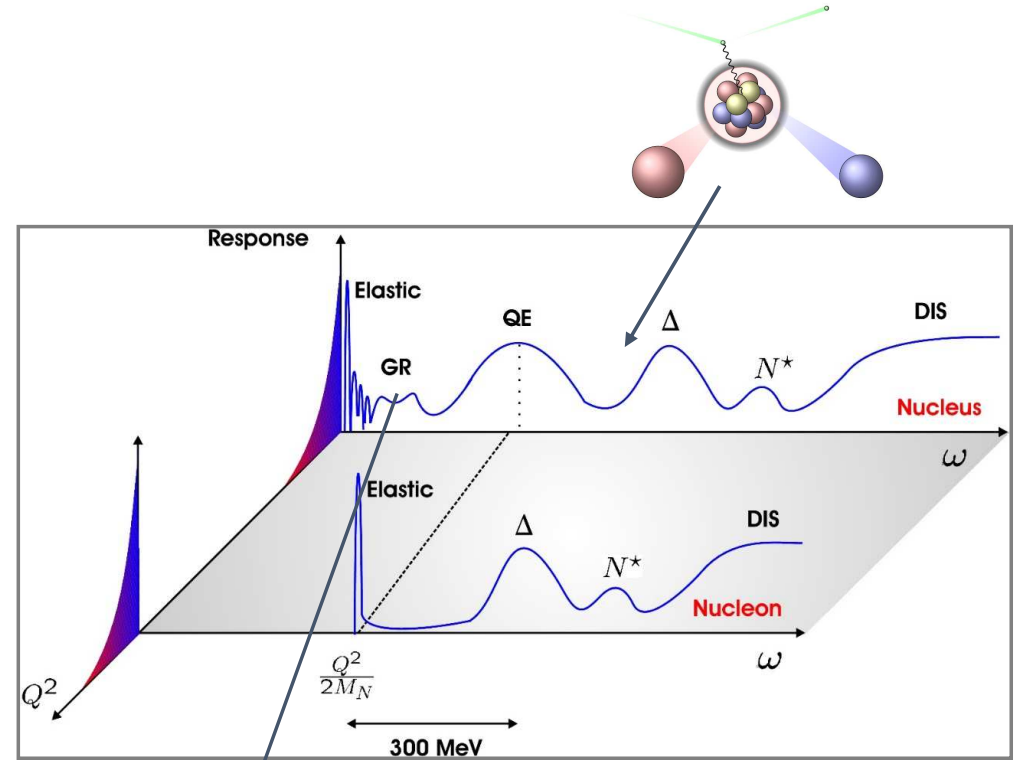
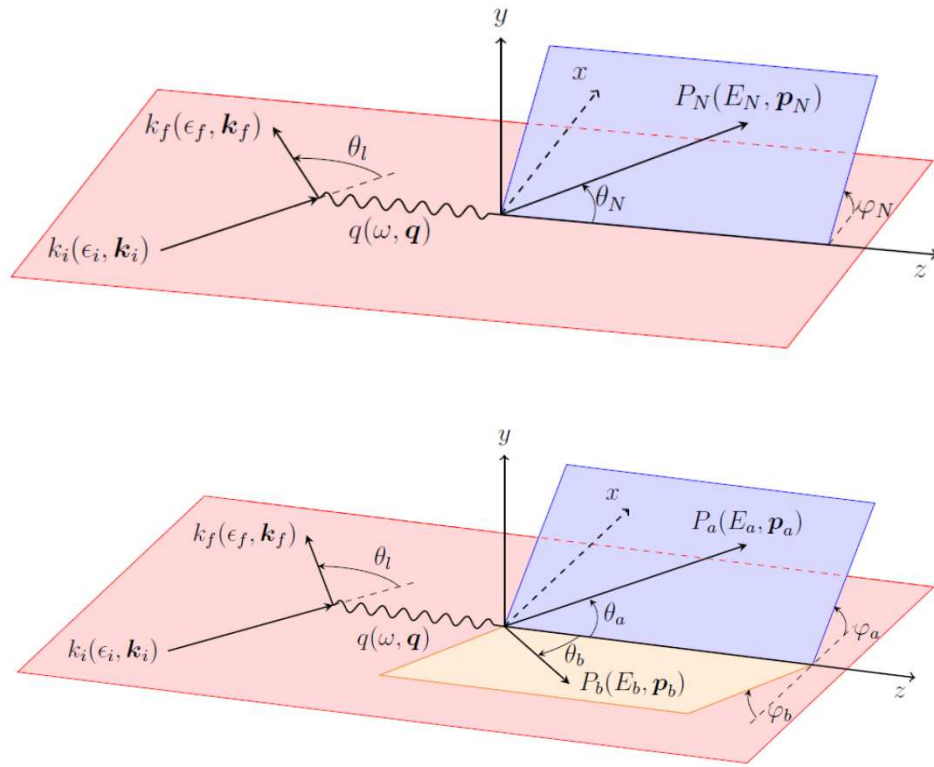
Natalie Jachowicz, T. Van Cuyck, A. Nikolakopoulos, N. Van Dessel, R. González-Jimenez, V. Pandey

Outline

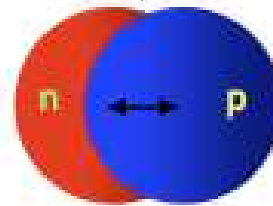
- Detailed microscopic cross sections calculations for QE(-like) scattering
- influence of long-range correlations
- influence of short-range correlations in 1- and 2-nucleon knockout processes
- Influence of seagull and pion-in-flight MEC contributions

Neutrino-hadron scattering

Dip region : multinucleon mechanisms

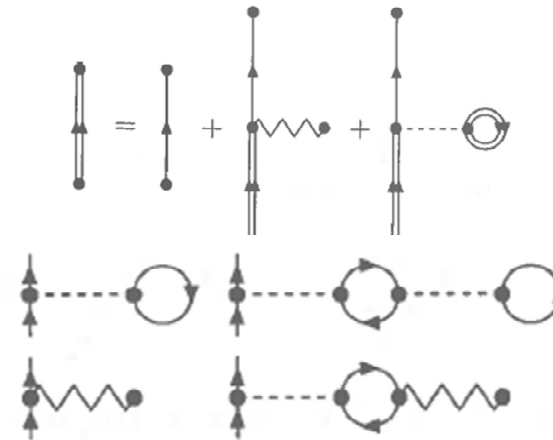
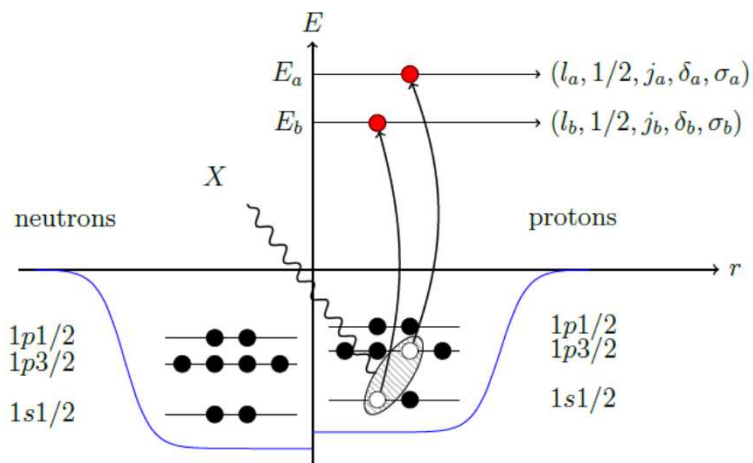
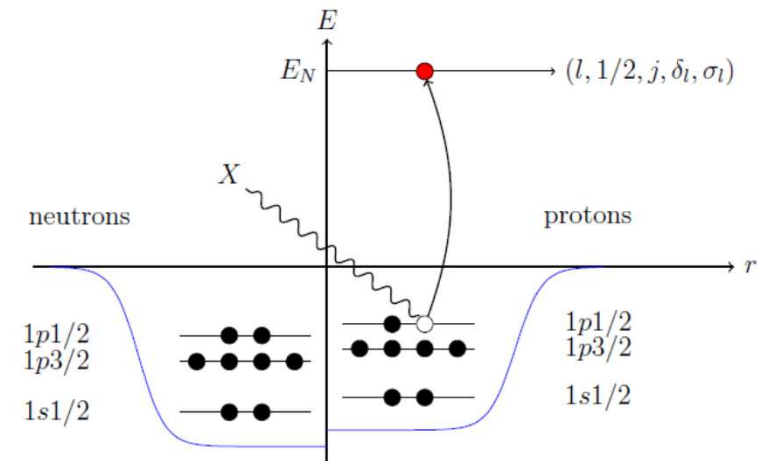


e.g.



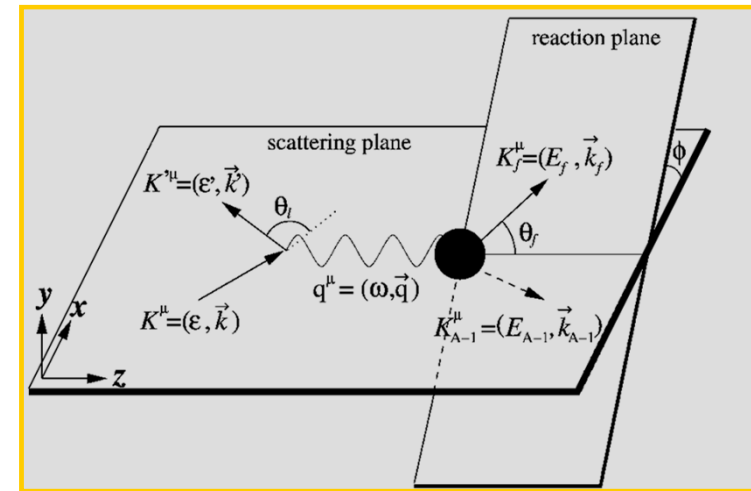
Cross section calculations

- Starting point : mean-field nucleus with Hartree-Fock single-particle wave functions
- Skyrme SkE2 force used to build the potential
- Pauli blocking
- Binding
- **Mean field already contains correlations !**



Neutrino-nucleus interactions

$$\hat{H}_W = \frac{G}{\sqrt{2}} \int d\vec{x} \hat{j}_{\mu,lepton}(\vec{x}) \hat{j}^{\mu,hadron}(\vec{x})$$



Hadron current

$$J^\mu = F_1(Q^2)\gamma^\mu + i\frac{\kappa}{2M_N}F_2(Q^2)\sigma^{\mu\nu}q_\nu + G_A(Q^2)\gamma^\mu\gamma_5 + \frac{1}{2M_N}G_P(Q^2)q^\mu\gamma_5$$

Lepton tensor

$$l_{\alpha\beta} \equiv \sum_{s,s'} \overline{[\bar{u}_l \gamma_\alpha (1 - \gamma_5) u_l]}^\dagger [\bar{u}_\nu \gamma_\beta (1 - \gamma_5) u_\nu]$$

$$\vec{J}_V^\alpha(\vec{x}) = \vec{J}_{convection}^\alpha(\vec{x}) + \vec{J}_{magnetization}^\alpha(\vec{x})$$

$$\text{with } \vec{J}_c^\alpha(\vec{x}) = \frac{1}{2Mi} \sum_{i=1}^A G_E^{i,\alpha} \left[\delta(\vec{x} - \vec{x}_i) \vec{\nabla}_i - \overleftarrow{\nabla}_i \delta(\vec{x} - \vec{x}_i) \right],$$

$$\vec{J}_m^\alpha(\vec{x}) = \frac{1}{2M} \sum_{i=1}^A G_M^{i,\alpha} \vec{\nabla} \times \vec{\sigma}_i \delta(\vec{x} - \vec{x}_i),$$

$$\vec{J}_A^\alpha(\vec{x}) = \sum_{i=1}^A G_A^{i,\alpha} \vec{\sigma}_i \delta(\vec{x} - \vec{x}_i),$$

$$J_V^{0,\alpha}(\vec{x}) = \rho_V^\alpha(\vec{x}) = \sum_{i=1}^A G_E^{i,\alpha} \delta(\vec{x} - \vec{x}_i),$$

$$J_A^{0,\alpha}(\vec{x}) = \rho_A^\alpha(\vec{x}) = \frac{1}{2Mi} \sum_{i=1}^A G_A^{i,\alpha} \vec{\sigma}_i \cdot \left[\delta(\vec{x} - \vec{x}_i) \vec{\nabla}_i - \overleftarrow{\nabla}_i \delta(\vec{x} - \vec{x}_i) \right]$$

$$J_P^{0,\alpha}(\vec{x}) = \rho_P^\alpha(\vec{x}) = \frac{m_\mu}{2M} \sum_{i=1}^A G_P^{i,\alpha} \vec{\nabla} \cdot \vec{\sigma}_i \delta(\vec{x} - \vec{x}_i)$$

for NC reactions

$$G_E^{V,0} = \left(\frac{1}{2} - \sin^2 \theta_W \right) \tau_3 - \sin^2 \theta_W,$$

$$G_M^{V,0} = \left(\frac{1}{2} - \sin^2 \theta_W \right) (\mu_p - \mu_n) \tau_3 - \sin^2 \theta_W (\mu_p + \mu_n)$$

$$G^{A,0} = g_a \frac{\tau_3}{2} = -\frac{1.262}{2} \tau_3$$

for CC reactions

$$G_E^{V,\pm} = \tau_\pm$$

$$G_M^{V,\pm} = (\mu_p - \mu_n) \tau_\pm$$

$$G^{A,\pm} = g_a \tau_\pm = -1.262 \tau_\pm$$

$G = (1 + Q^2/M^2)^{-2}$ Q^2 dependence : dipole parametrization or BBBA07 :

Inclusive QE 1-nucleon knockout cross sections

$$\frac{d^2\sigma}{d\Omega d\omega} = (2\pi)^4 k_f \varepsilon_f \sum_{s_f, s_i} \frac{1}{2J_i + 1} \sum_{M_f, M_i} |\langle f | \hat{H}_W | i \rangle|^2$$

$$\left(\frac{d^2\sigma_{i \rightarrow f}}{d\Omega d\omega} \right)_{\nu} = \frac{G^2 \varepsilon_f^2}{\pi} \frac{2 \cos^2 \left(\frac{\theta}{2} \right)}{2J_i + 1} \left[\sum_{J=0}^{\infty} \sigma_{CL}^J + \sum_{J=1}^{\infty} \sigma_T^J \right]$$

$$\sigma_{CL}^J = \left| \left\langle J_f \left\| \hat{\mathcal{M}}_J(\kappa) + \frac{\omega}{|\vec{q}|} \hat{\mathcal{L}}_J(\kappa) \right\| J_i \right\rangle \right|^2$$

$$\sigma_T^J = \left(-\frac{q_\mu^2}{2|\vec{q}|^2} + \tan^2 \left(\frac{\theta}{2} \right) \right) \left[\left| \left\langle J_f \left\| \hat{\mathcal{J}}_J^{mag}(\kappa) \right\| J_i \right\rangle \right|^2 + \left| \left\langle J_f \left\| \hat{\mathcal{J}}_J^{el}(\kappa) \right\| J_i \right\rangle \right|^2 \right]$$

$$\mp \tan \left(\frac{\theta}{2} \right) \sqrt{-\frac{q_\mu^2}{|\vec{q}|^2} + \tan^2 \left(\frac{\theta}{2} \right)} \left[2\Re \left(\left\langle J_f \left\| \hat{\mathcal{J}}_J^{mag}(\kappa) \right\| J_i \right\rangle \left\langle J_f \left\| \hat{\mathcal{J}}_J^{el}(\kappa) \right\| J_i \right\rangle^* \right) \right]$$

2-nucleon knockout cross sections

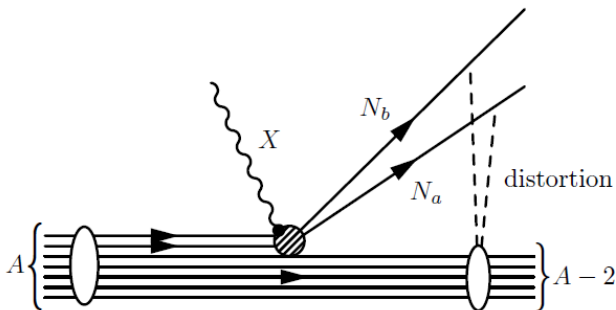
2-nucleon knockout :

$$\frac{d\sigma^X}{dE_f d\Omega_f dT_b d\Omega_b d\Omega_a} = \frac{p_a p_b E_a E_b}{(2\pi)^6} g_{rec}^{-1} \sigma^X \zeta$$

$$\times [v_{CC} W_{CC} + v_{CL} W_{CL} + v_{LL} W_{LL} + v_T W_T + v_{TT} W_{TT} + v_{TC} W_{TC} + v_{TL} W_{TL} + h(v_{T'} W_{T'} + v_{TC'} W_{TC'} + v_{TL'} W_{TL'})],$$

with :

$$\mathcal{J}_\lambda = \langle \Phi_f^{(A-2)}(E^{exc}, J_R M_R); \mathbf{p}_a m_{s_a}; \mathbf{p}_b m_{s_b} | \hat{J}_\lambda(\mathbf{q}) | \Phi_{gs} \rangle$$



$$|\Phi^{2p2h}\rangle = |\Phi_f^{(A-2)}(E^{exc}, J_R M_R); \mathbf{p}_a m_{s_a}; \mathbf{p}_b m_{s_b}\rangle_{as}$$

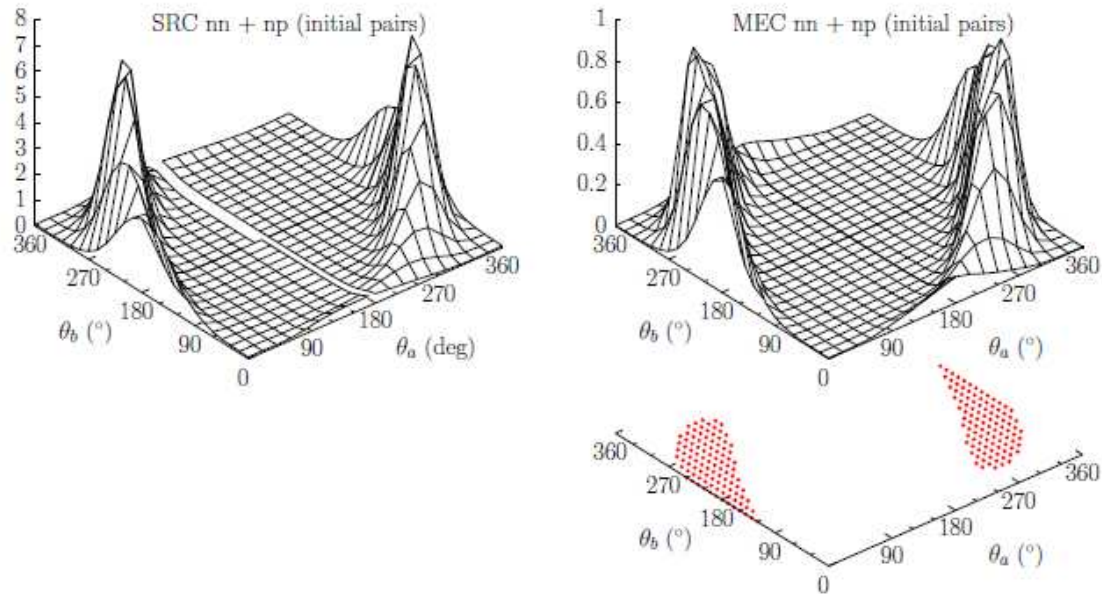
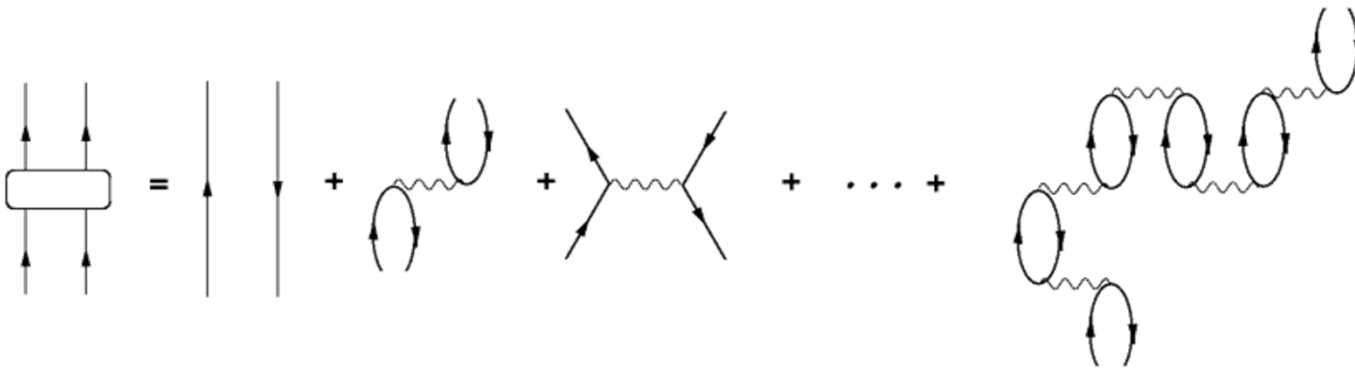


Figure 4.5: The $^{12}\text{C}(\nu_\mu, \mu^- N_a N_b)$ cross section ($N_a = p, N_b = p', n$) at $\epsilon_{\nu_\mu} = 750$ MeV, $\epsilon_\mu = 550$ MeV, $\theta_\mu = 15^\circ$ and $T_p = 50$ MeV for in-plane kinematics. Left with SRCs, right with MECs, the bottom plot shows the (θ_a, θ_b) regions with $P_{12} < 300$ MeV/c.

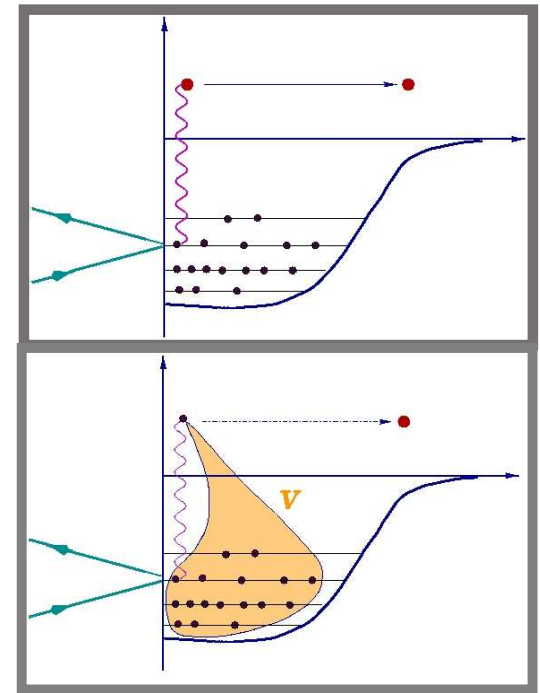
- Strength residing in restricted part of phase space
- $p_b \approx p_b^{ave}$
- Quasi-deuteron kinematics

Long-range correlations : Continuum RPA

- Green's function approach
- Skyrme SkE2 residual interaction
- self-consistent calculations



$$\Pi^{(RPA)}(x_1, x_2; \omega) = \Pi^{(0)}(x_1, x_2; \omega) + \frac{1}{\hbar} \int dx \int dx' \Pi^{(0)}(x_1, x; \omega) \tilde{V}(x, x') \Pi^{(RPA)}(x', x_2; \omega)$$



$$|\Psi_{RPA}\rangle = \sum_c \{ X_{(\Psi,C)} |ph^{-1}\rangle - Y_{(\Psi,C)} |hp^{-1}\rangle \} + \dots$$

Solving the RPA equations in coordinate space :

$$\begin{aligned}
 |\Psi_C(E)\rangle &= |ph^{-1}(E)\rangle + \int dx_1 \int dx_2 \tilde{V}(x_1, x_2) \\
 &\sum_{c'} \mathcal{P} \int d\varepsilon_{p'} \left[\frac{\psi_{h'}(x_1) \psi_{p'}^\dagger(x_1, \varepsilon_{p'})}{E - \varepsilon_{p'h'}} |p'h'^{-1}(\varepsilon_{p'h'})\rangle \right. \\
 &\quad \left. - \frac{\psi_{h'}^\dagger(x_1) \psi_{p'}(x_1, \varepsilon_{p'})}{E + \varepsilon_{p'h'}} |h'p'^{-1}(-\varepsilon_{p'h'})\rangle \right] \langle \Psi_0 | \hat{\psi}^\dagger(x_2) \hat{\psi}(x_2) | \Psi_C(E) \rangle
 \end{aligned}$$

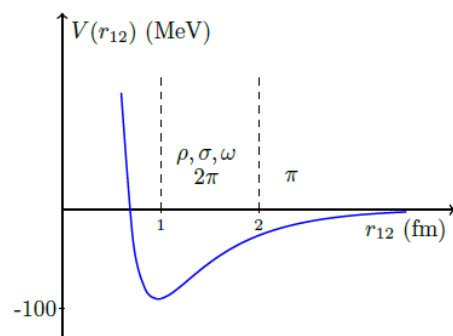
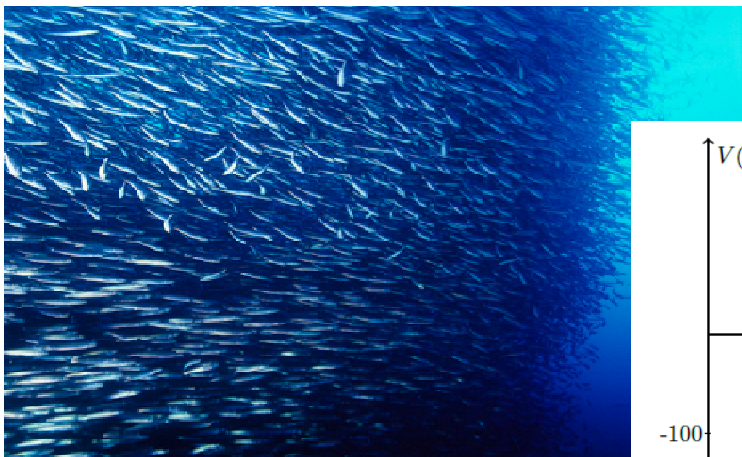
What we really need is transition densities :

$$\begin{aligned}
 \langle \Psi_0 || X_{\eta J} || \Psi_C(J; E) \rangle_r &= - \langle h || X_{\eta J} || p(\varepsilon_{ph}) \rangle_r \\
 &+ \sum_{\mu, \nu} \int dr_1 \int dr_2 U_{\mu\nu}^J(r_1, r_2) \mathcal{R} \left(R_{\eta\mu; J}^{(0)}(r, r_1; E) \right) \langle \Psi_0 || X_{\nu J} || \Psi_C(J; E) \rangle_{r_2}
 \end{aligned}$$

So in the end we have to solve a set of coupled equations, that after discretizing on a mesh in coordinate space, translates into a matrix inversion for the transition densities:

$$\rho_C^{RPA} = - \frac{1}{1 - RU} \rho_C^{HF}$$

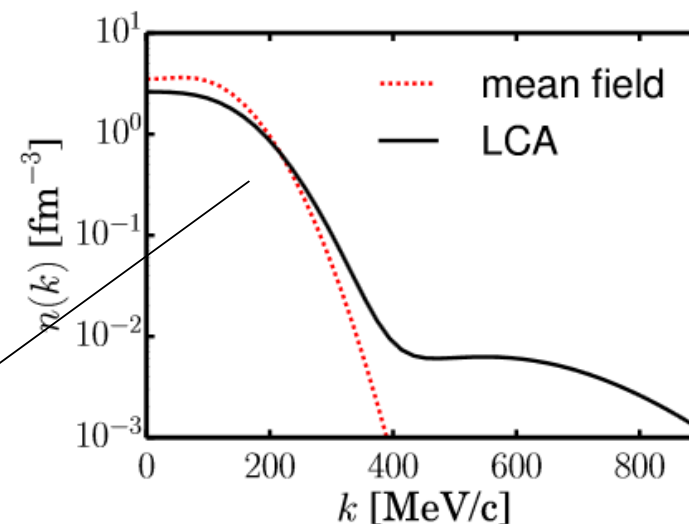
Short-range correlations



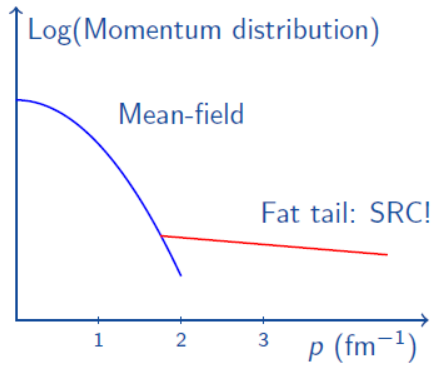
- SRC : short-range repulsive, tensor component of the nuclear force
- Individual nucleons receive large momenta compared to the Fermi momentum

- The short-range repulsive character of the nuclear force, which correlates with the Pauli exclusion principle, results in a large mean free path of the nucleons with respect to the size of the nucleus
- In an independent particle model nucleons move independently from each other in a mean field
- This approach fails to capture short-range features of nucleon-nucleon correlations

IPM single-particle orbitals are depleted by SRC and higher energy levels are populated



Short-range correlations

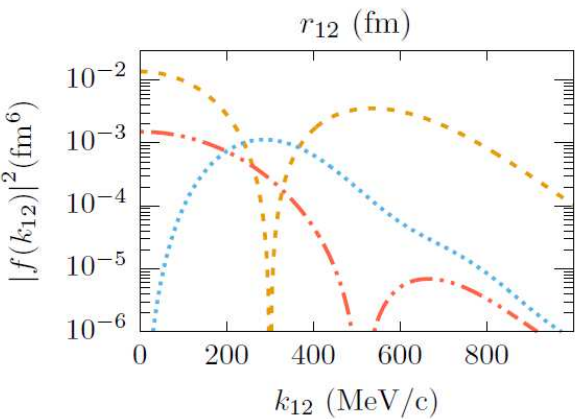
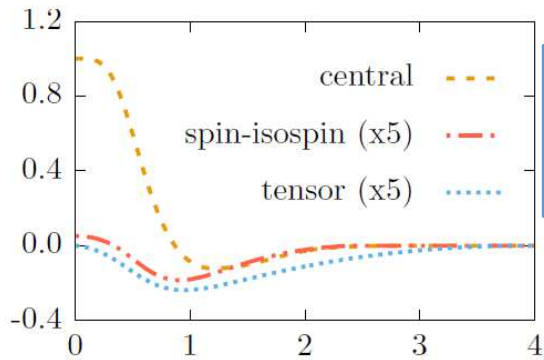


$$|\Psi\rangle = \frac{1}{\sqrt{\mathcal{N}}} \hat{\mathcal{G}} |\Phi\rangle \quad \text{with} \quad \hat{\mathcal{G}} \approx \hat{\mathcal{S}} \left(\prod_{i<j}^A [1 + \hat{l}(i, j)] \right)$$

$$\hat{l}(i, j) = -g_c(r_{ij}) + f_{\sigma\tau}(r_{ij}) (\vec{\sigma}_i \cdot \vec{\sigma}_j) (\vec{\tau}_i \cdot \vec{\tau}_j) + f_{t\tau}(r_{ij}) \hat{S}_{ij} (\vec{\tau}_i \cdot \vec{\tau}_j),$$

Shifting the complexity induced by correlations from the wave functions to the operators

$$\langle \Psi_f | \hat{J}_\mu^{\text{nucl}} | \Psi_i \rangle = \frac{1}{\sqrt{\mathcal{N}_i \mathcal{N}_f}} \langle \Phi_f | \hat{J}_\mu^{\text{eff}} | \Phi_i \rangle$$

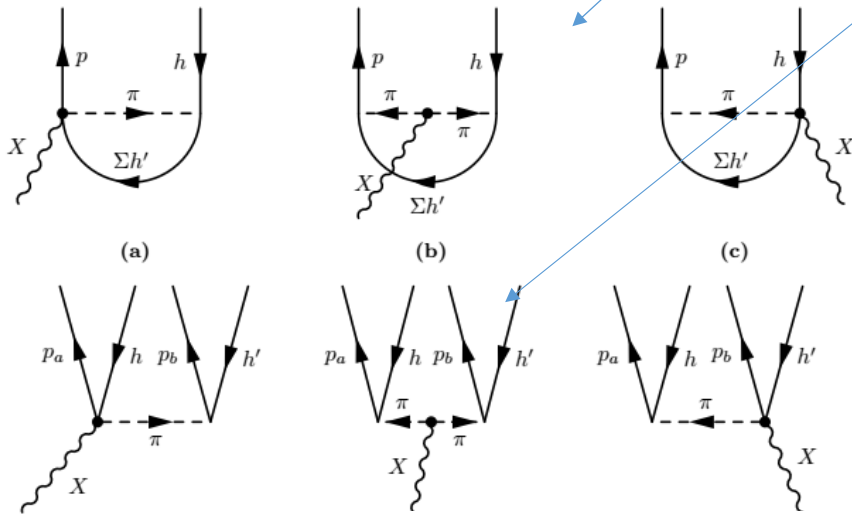


$$\hat{J}_\mu^{\text{eff}} \approx \sum_{i=1}^A \hat{J}_\mu^{[1]}(i) + \sum_{i<j}^A \hat{J}_\mu^{[1],\text{in}}(i, j) + \left[\sum_{i<j}^A \hat{J}_\mu^{[1],\text{in}}(i, j) \right]^\dagger$$

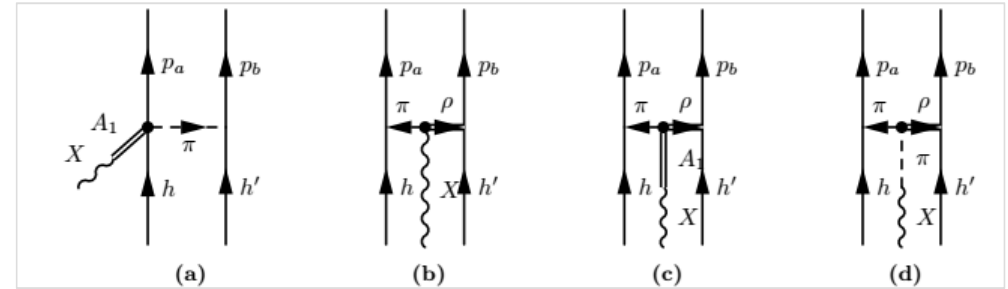
$$\hat{J}_\mu^{[1],\text{in}}(i, j) = \left[\hat{J}_\mu^{[1]}(i) + \hat{J}_\mu^{[1]}(j) \right] \hat{l}(i, j)$$

Gearheart (1994) Pieper (1992)

III. MEC in 1p1h and 2p2h

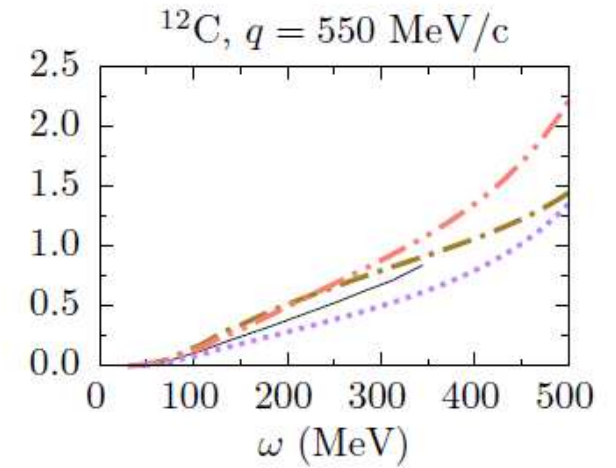
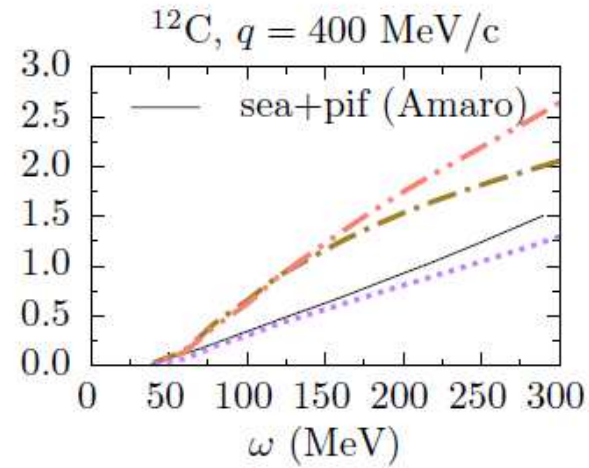
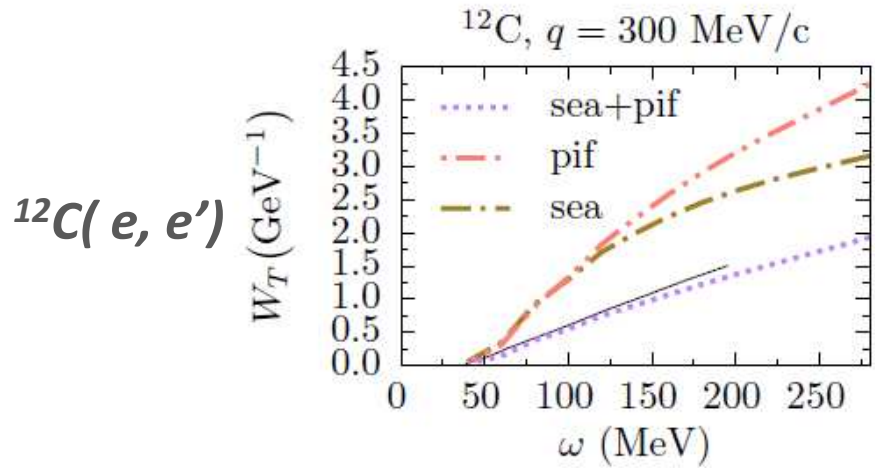


Axial contributions :

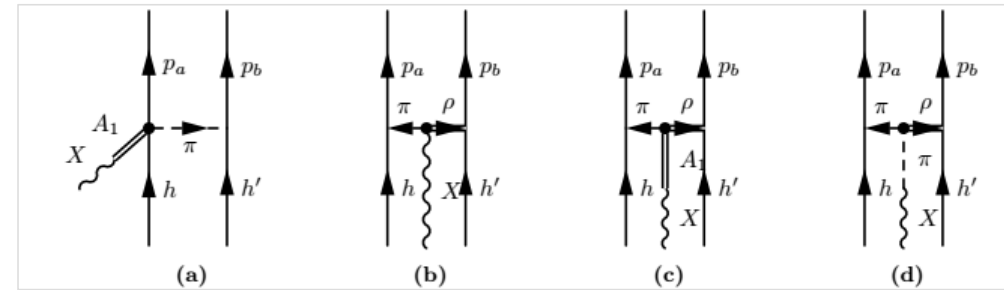


$$\hat{\rho}_A^{[2],\text{axi}}(\mathbf{q}) = \frac{i}{g_A} \left(\frac{f_{\pi NN}}{m_\pi} \right)^2 (\mathbf{I}_V) \left(F_\pi(q_2^2) \Gamma_\pi^2(q_2^2) \frac{\boldsymbol{\sigma}_2 \cdot \mathbf{q}_2}{q_2^2 + m_\pi^2} - F_\pi(q_1^2) \Gamma_\pi^2(q_1^2) \frac{\boldsymbol{\sigma}_1 \cdot \mathbf{q}_1}{q_1^2 + m_\pi^2} \right)$$

I. Towner, Nucl. Phys.A542, 631 (1992)

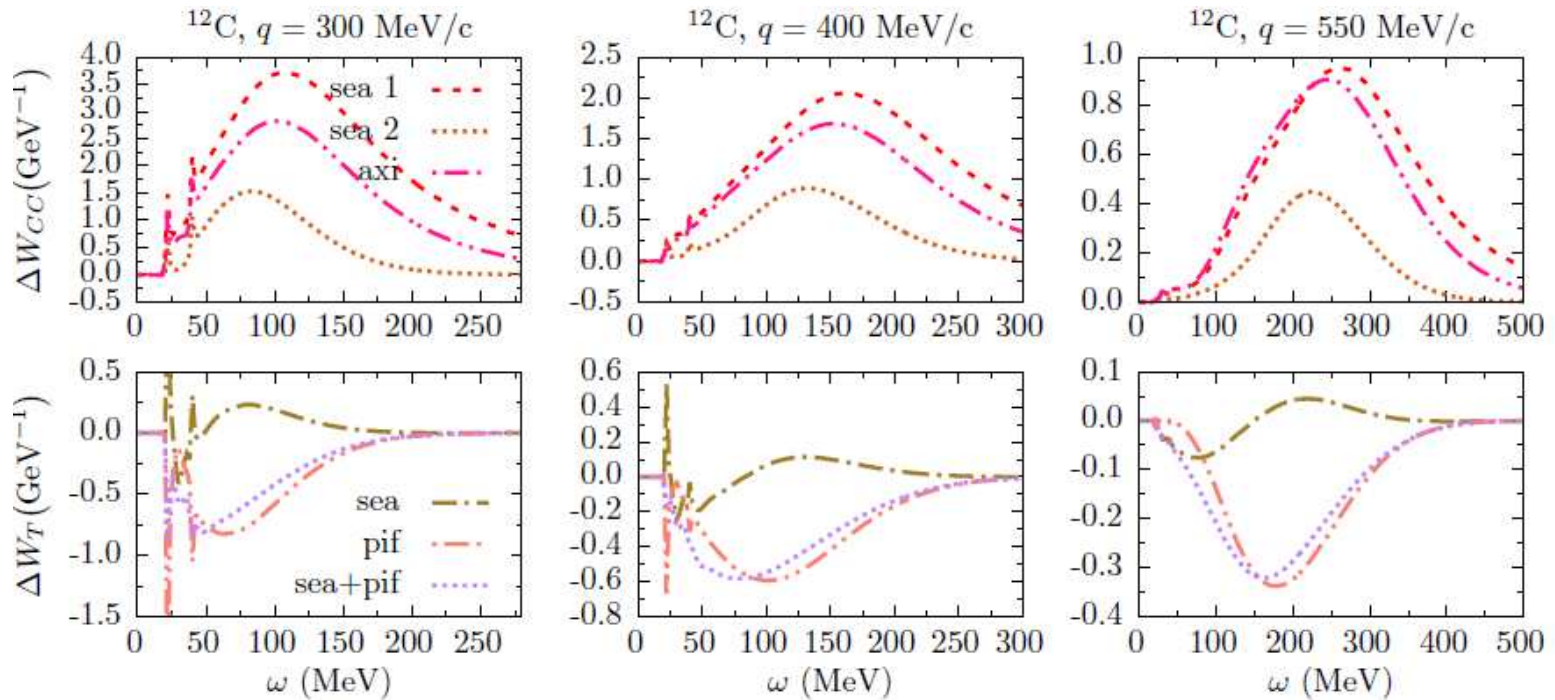


- Only seagull have axial counterpart
- timelike
- Partially constrained by PCAC
- Non-relativistic reduction not unambiguous



I. Towner, Nucl. Phys.A542, 631 (1992)

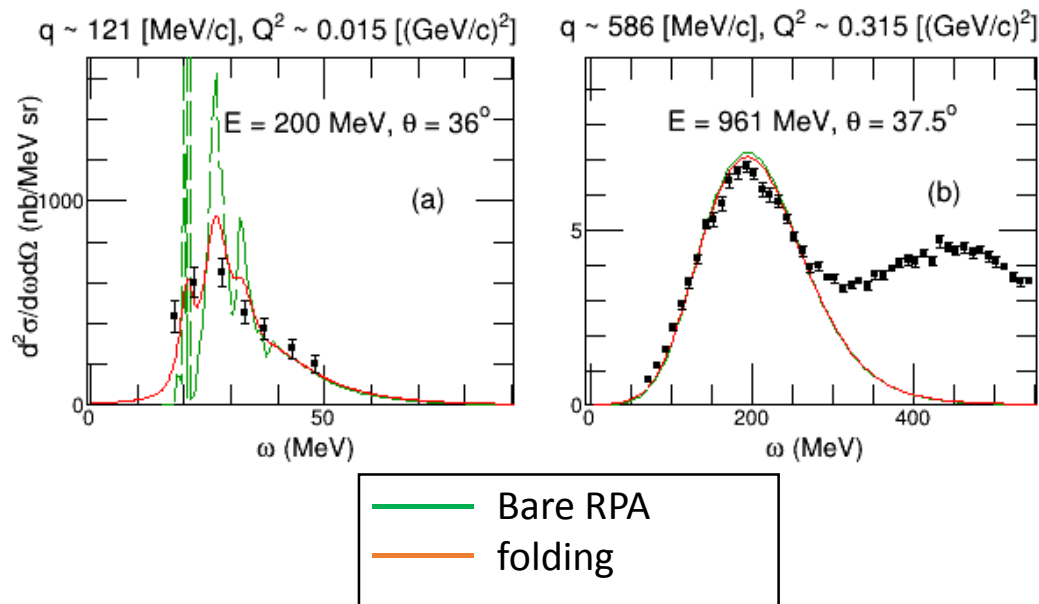
$$\hat{\rho}_A^{[2],\text{axi}}(\mathbf{q}) = \frac{i}{g_A} \left(\frac{f_{\pi NN}}{m_\pi} \right)^2 (I_V) \left(F_\pi(q_2^2) \Gamma_\pi^2(q_2^2) \frac{\boldsymbol{\sigma}_2 \cdot \mathbf{q}_2}{q_2^2 + m_\pi^2} - F_\pi(q_1^2) \Gamma_\pi^2(q_1^2) \frac{\boldsymbol{\sigma}_1 \cdot \mathbf{q}_1}{q_1^2 + m_\pi^2} \right)$$



- Final state interactions :

- taken into account through the calculations of the wave function of the outgoing nucleon in the (real) nuclear potential generated using the Skyrme force

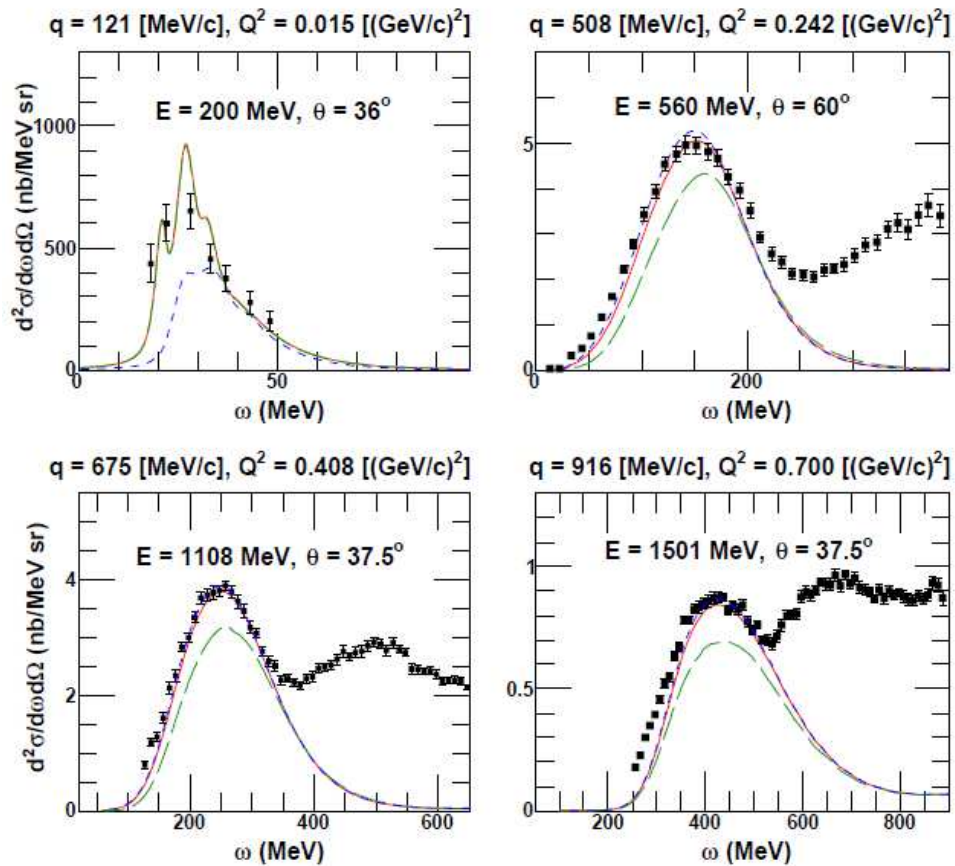
- influence of the spreading width of the particle states is implemented through a folding procedure



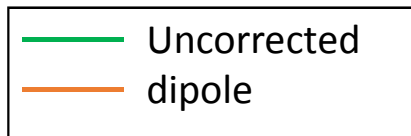
$$R'(q, \omega') = \int_{-\infty}^{\infty} d\omega R(q, \omega) L(\omega, \omega'),$$

$$L(\omega, \omega') = \frac{1}{2\pi} \left[\frac{\Gamma}{(\omega - \omega')^2 + (\Gamma/2)^2} \right].$$

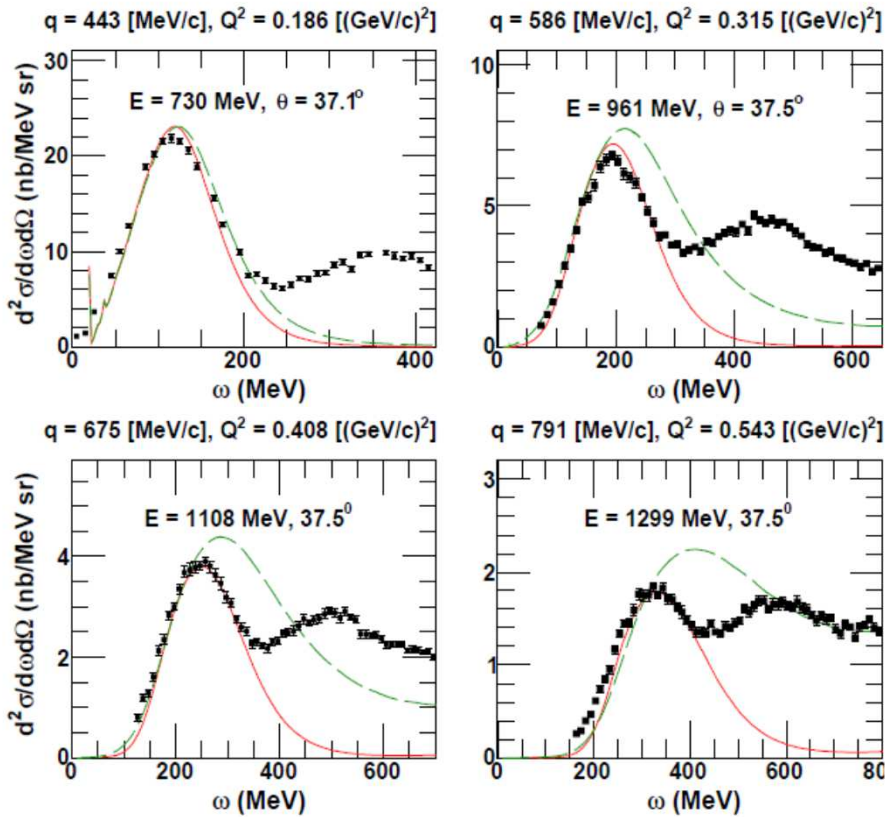
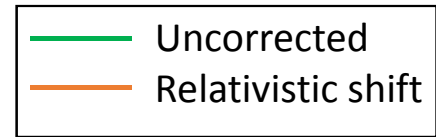
•Regularization of the residual interaction :



$$V(Q^2) \rightarrow V(Q^2 = 0) \frac{1}{\left(1 + \frac{Q^2}{\Lambda^2}\right)^2}$$



•Relativistic corrections at higher energies (J. Jeschonnek and T. Donnelly, PRC57, 2438 (1998)):



Shift :

$$\lambda \rightarrow \lambda(\lambda + 1) \quad \lambda = \omega/2M_N$$

- The outgoing nucleon obtains the correct relativistic momentum
- $$p = \sqrt{T^2 + 2MT}$$
- Shifts the QE peak to the right relativistic position

Boost :

$$R_{CC}^V(q, \omega) \rightarrow \frac{q^2}{q^2 - \omega^2} R_{CC}^V(q, \omega),$$

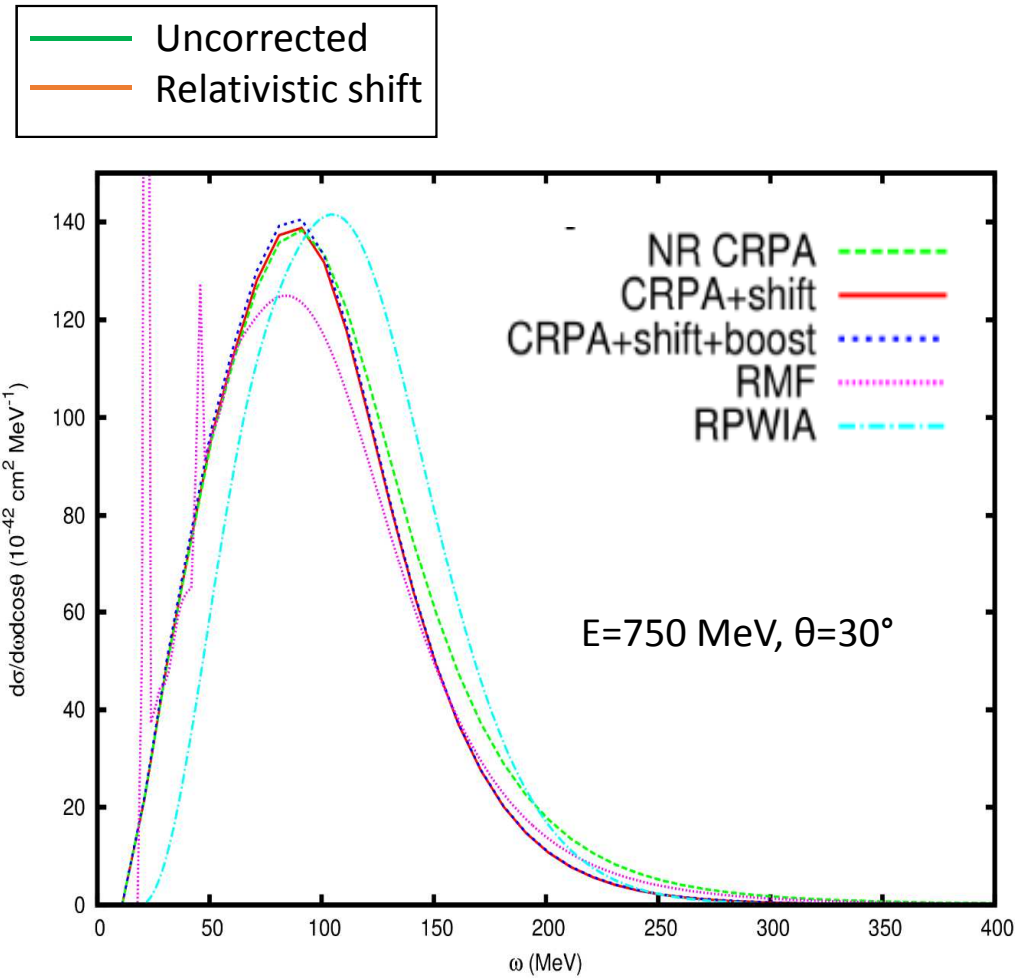
$$R_{LL}^A(q, \omega) \rightarrow \left(1 + \frac{q^2 - \omega^2}{4m^2}\right) R_{LL}^A(q, \omega),$$

$$R_{T}^V(q, \omega) \rightarrow \frac{q^2 - \omega^2}{q^2} R_{T}^V(q, \omega),$$

$$R_{T}^A(q, \omega) \rightarrow \left(1 + \frac{q^2 - \omega^2}{4m^2}\right) R_{T}^A(q, \omega),$$

$$R_{T'}^{VA}(q, \omega) \rightarrow \sqrt{\frac{q^2 - \omega^2}{q^2}} \sqrt{1 + \frac{q^2 - \omega^2}{4m^2}} R_{T'}^{VA}(q, \omega).$$

- Relativistic corrections at higher energies (J. Jeschonnek and T. Donnelly, PRC57, 2438 (1998)):



Shift :

$$\lambda \rightarrow \lambda(\lambda + 1) \quad \lambda = \omega/2M_N$$

The outgoing nucleon obtains the correct relativistic momentum

$$p = \sqrt{T^2 + 2MT}$$

Shifts the QE peak to the right relativistic position

Boost :

$$R_{CC}^V(q, \omega) \rightarrow \frac{q^2}{q^2 - \omega^2} R_{CC}^V(q, \omega),$$

$$R_{LL}^A(q, \omega) \rightarrow \left(1 + \frac{q^2 - \omega^2}{4m^2}\right) R_{LL}^A(q, \omega),$$

$$R_T^V(q, \omega) \rightarrow \frac{q^2 - \omega^2}{q^2} R_T^V(q, \omega),$$

$$R_T^A(q, \omega) \rightarrow \left(1 + \frac{q^2 - \omega^2}{4m^2}\right) R_T^A(q, \omega),$$

$$R_{T'}^{VA}(q, \omega) \rightarrow \sqrt{\frac{q^2 - \omega^2}{q^2}} \sqrt{1 + \frac{q^2 - \omega^2}{4m^2}} R_{T'}^{VA}(q, \omega).$$

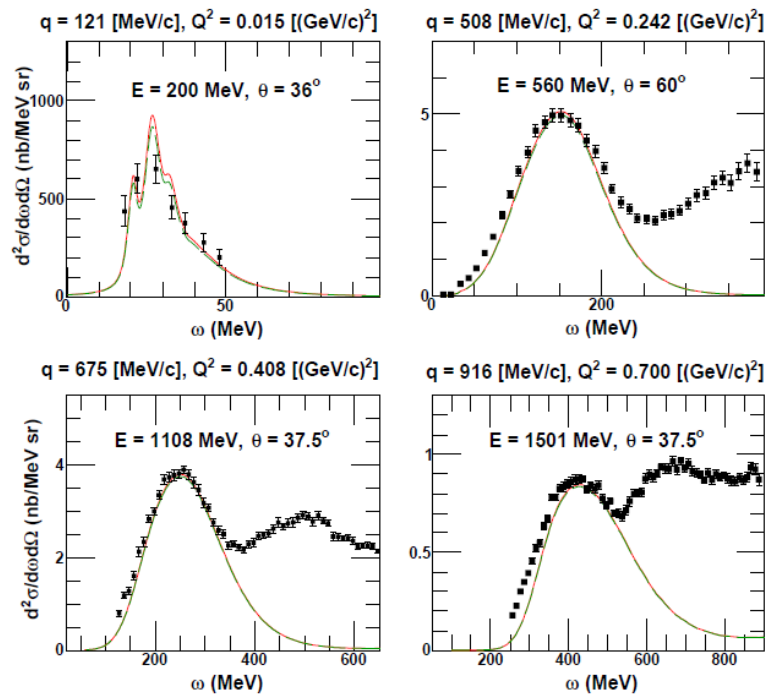
•Coulomb correction for the outgoing lepton in charged-current interactions :

✓ Low energies : Fermi function

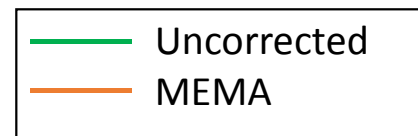
$$F(Z', E) = \frac{2\pi\eta}{1 - e^{-2\pi\eta}} \quad \eta \sim \mp Z' \alpha$$

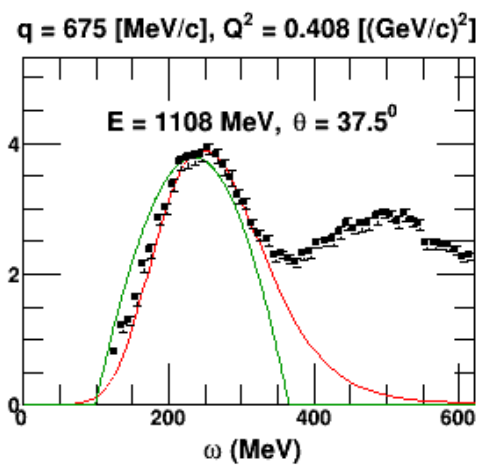
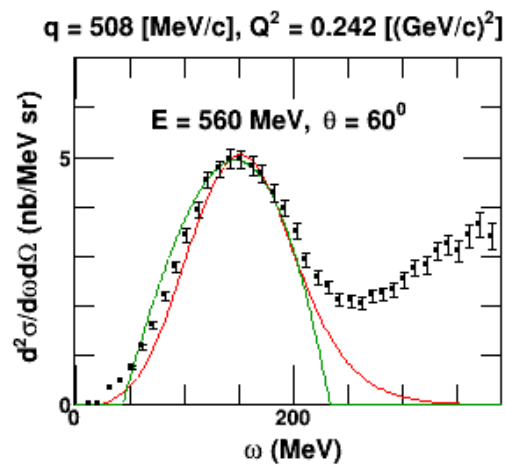
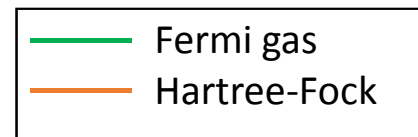
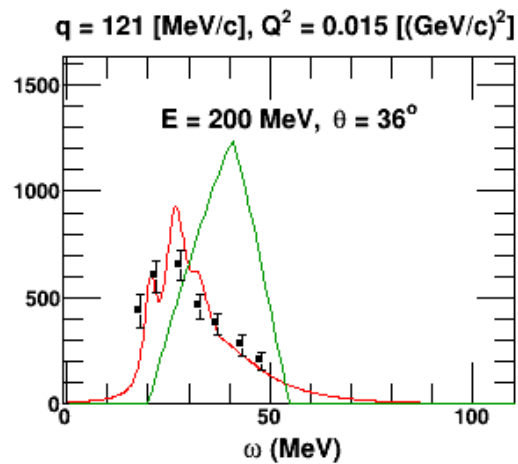
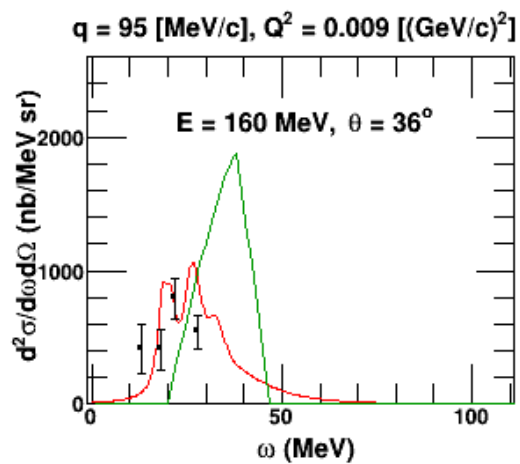
✓ High energies : modified effective momentum approximation (J. Engel, PRC57,2004 (1998))

$$q_{eff} = q + 1.5 \left(\frac{Z' \alpha \hbar c}{R} \right), \quad \Psi_l^{eff} = \zeta(Z', E, q) \Psi_l,$$

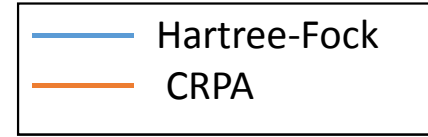


$$\zeta(Z', E, q) = \sqrt{\frac{q_{eff} E_{eff}}{q E}}$$

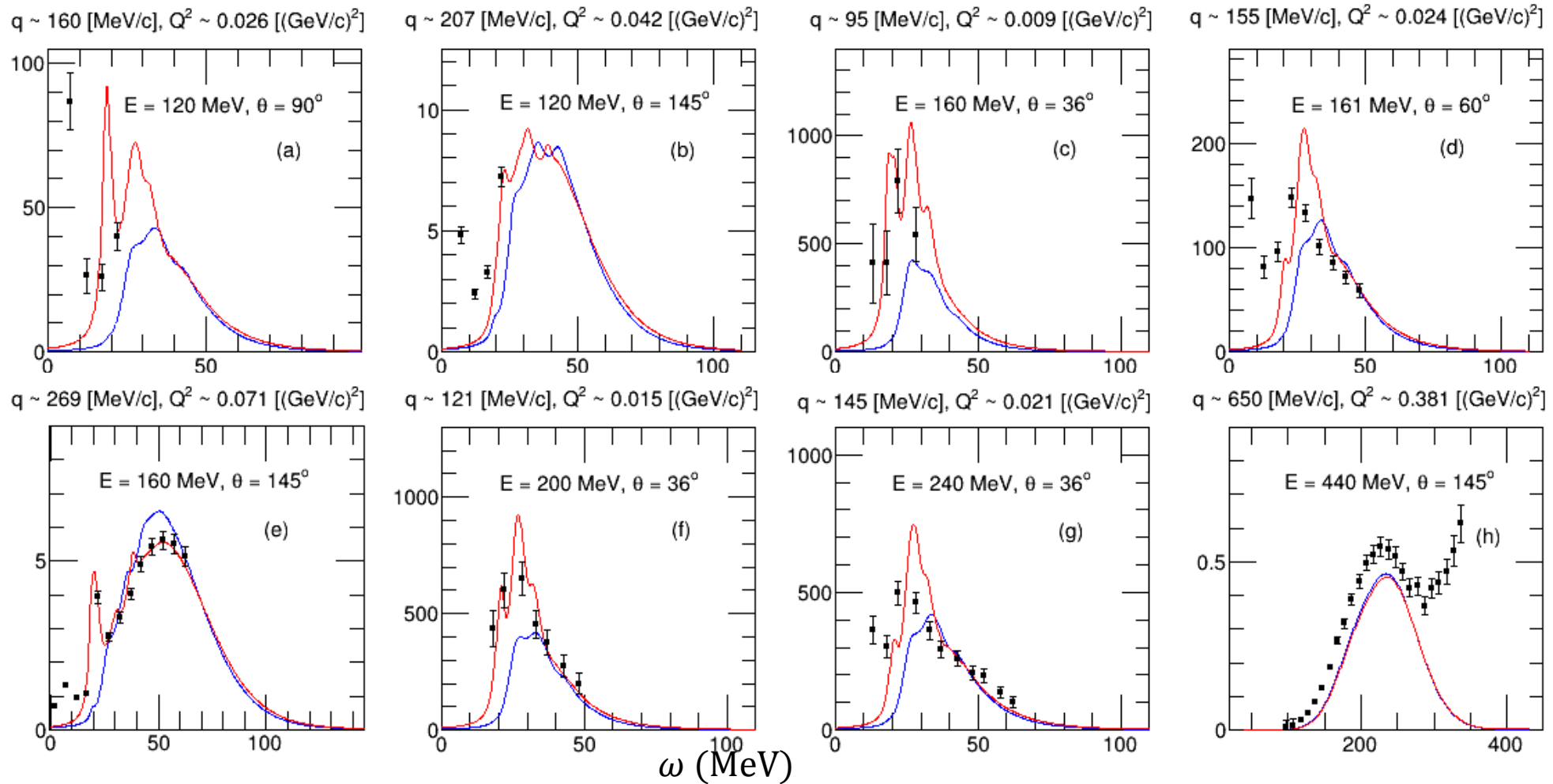




CRPA : Comparison with electron scattering data $^{12}\text{C}(e, e')$

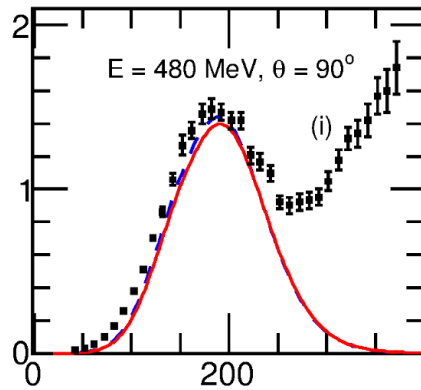


$d^2\sigma/d\omega d\Omega(\text{nb/MeV sr})$

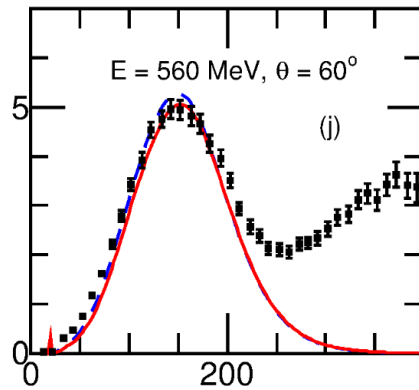


$d^2\sigma/d\omega d\Omega$ (nb/MeV sr)

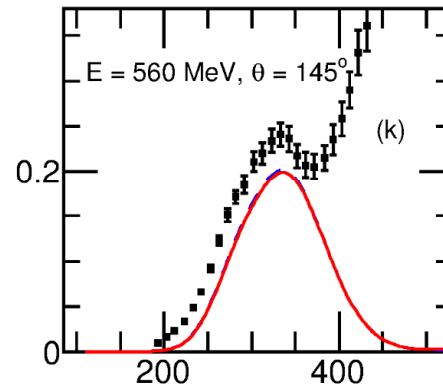
$q \sim 576$ [MeV/c], $Q^2 \sim 0.305$ [(GeV/c) 2]



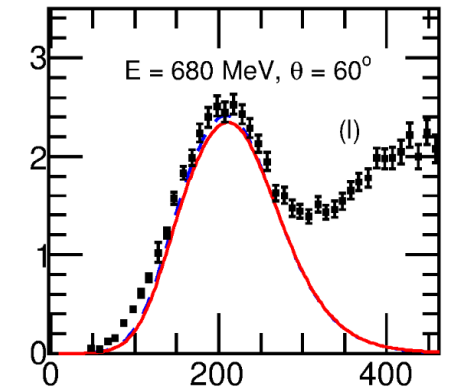
$q \sim 508$ [MeV/c], $Q^2 \sim 0.242$ [(GeV/c) 2]



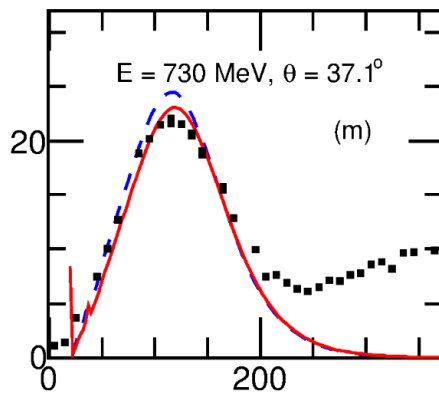
$q \sim 795$ [MeV/c], $Q^2 \sim 0.548$ [(GeV/c) 2]



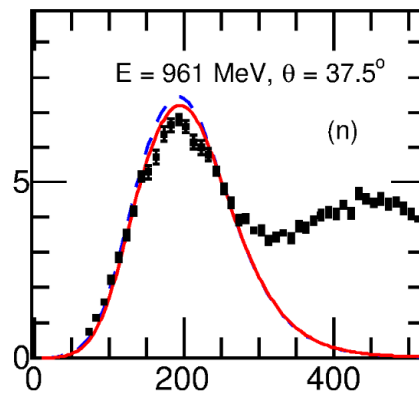
$q \sim 610$ [MeV/c], $Q^2 \sim 0.340$ [(GeV/c) 2]



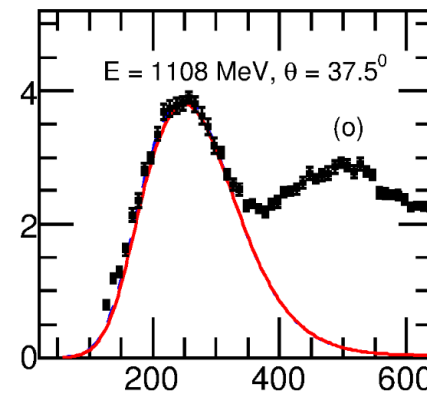
$q \sim 443$ [MeV/c], $Q^2 \sim 0.186$ [(GeV/c) 2]



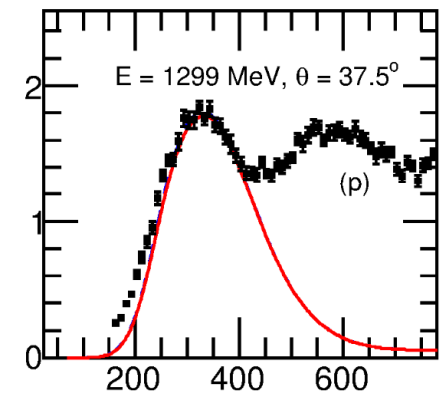
$q \sim 586$ [MeV/c], $Q^2 \sim 0.315$ [(GeV/c) 2]



$q \sim 675$ [MeV/c], $Q^2 \sim 0.408$ [(GeV/c) 2]



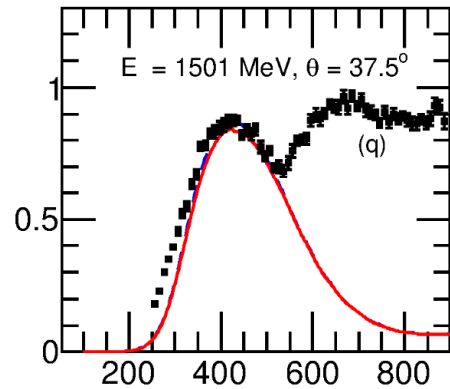
$q \sim 791$ [MeV/c], $Q^2 \sim 0.543$ [(GeV/c) 2]



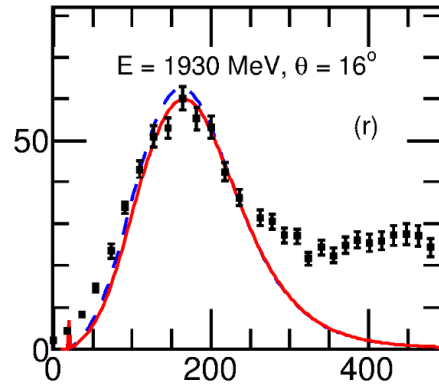
ω (MeV)

$d^2\sigma/d\omega d\Omega$ (nb/MeV sr)

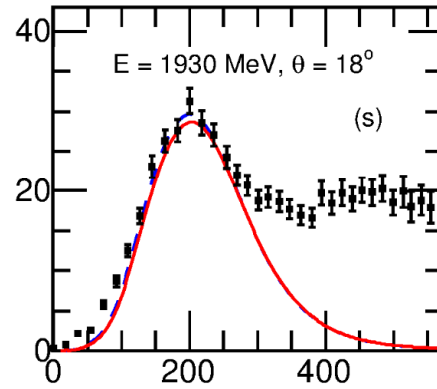
$q \sim 916$ [MeV/c], $Q^2 \sim 0.700$ [(GeV/c) 2]



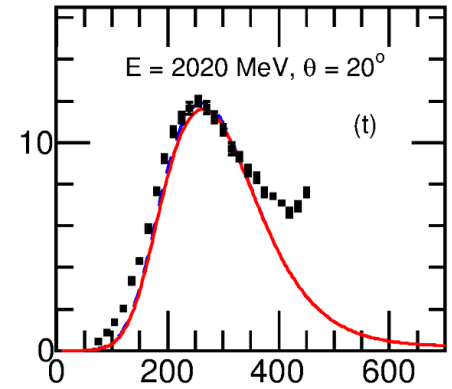
$q \sim 536$ [MeV/c], $Q^2 \sim 0.267$ [(GeV/c) 2]



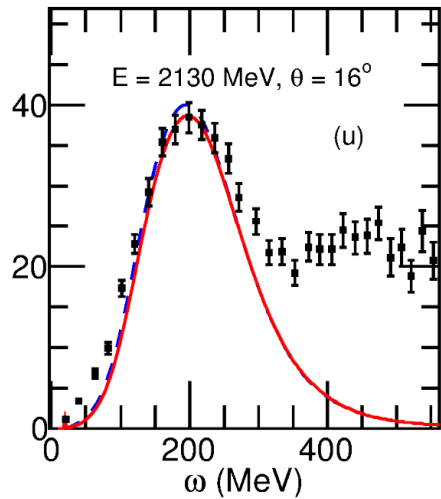
$q \sim 601$ [MeV/c], $Q^2 \sim 0.331$ [(GeV/c) 2]



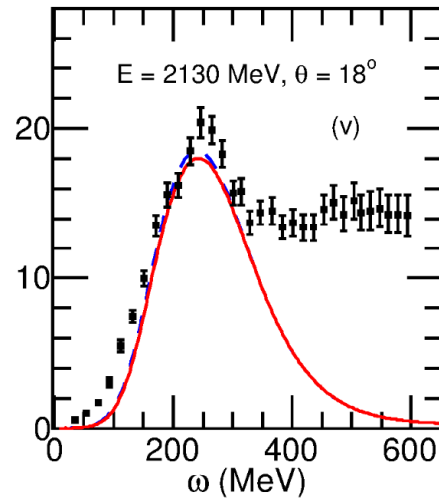
$q \sim 700$ [MeV/c], $Q^2 \sim 0.436$ [(GeV/c) 2]



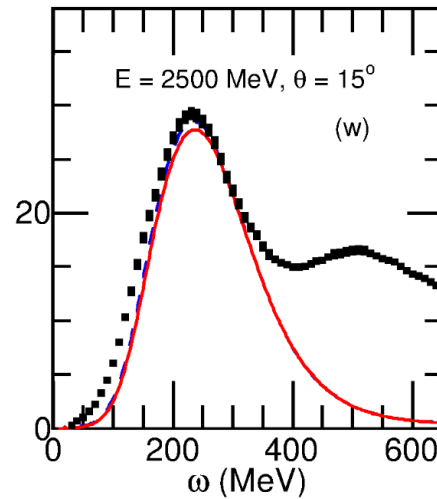
$q \sim 594$ [MeV/c], $Q^2 \sim 0.323$ [(GeV/c) 2]



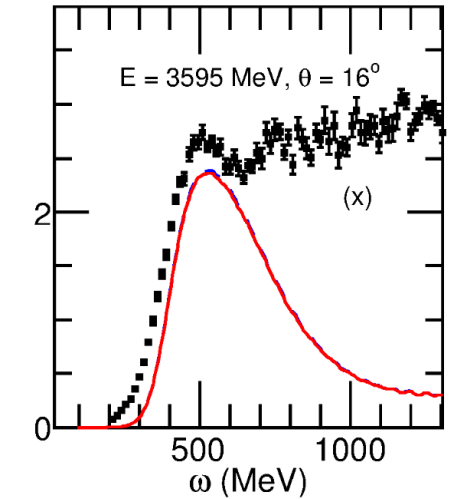
$q \sim 667$ [MeV/c], $Q^2 \sim 0.399$ [(GeV/c) 2]



$q \sim 658$ [MeV/c], $Q^2 \sim 0.391$ [(GeV/c) 2]

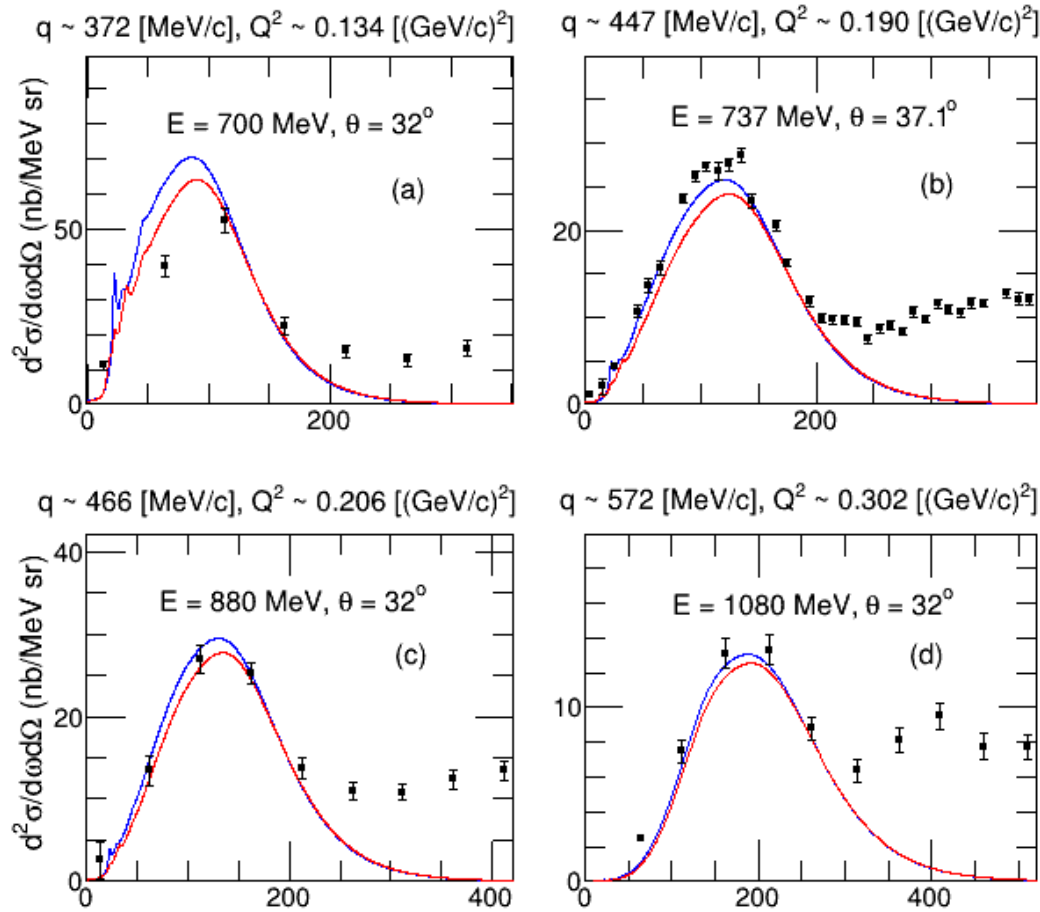


$q \sim 1043$ [MeV/c], $Q^2 \sim 0.872$ [(GeV/c) 2]



ω (MeV)

$^{16}\text{O}(e, e')$

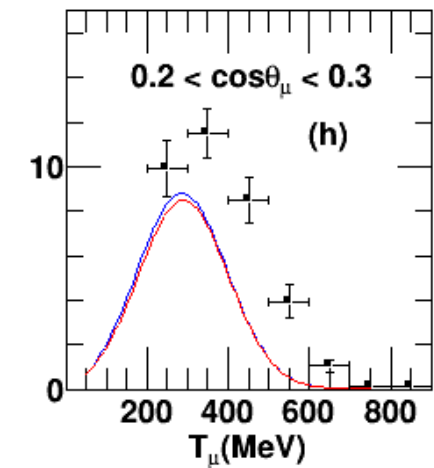
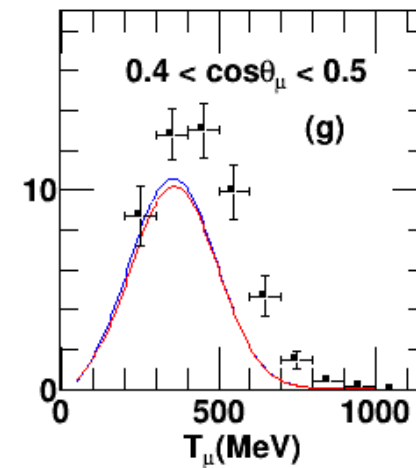
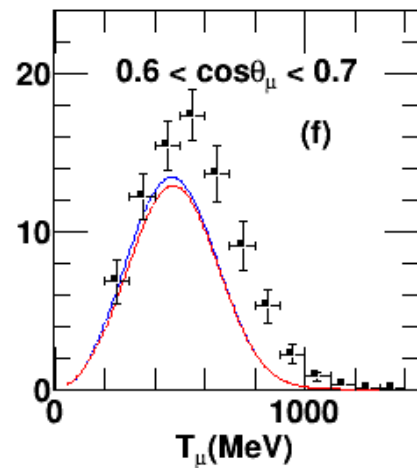
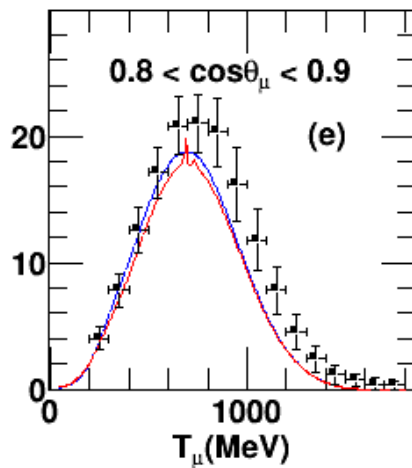
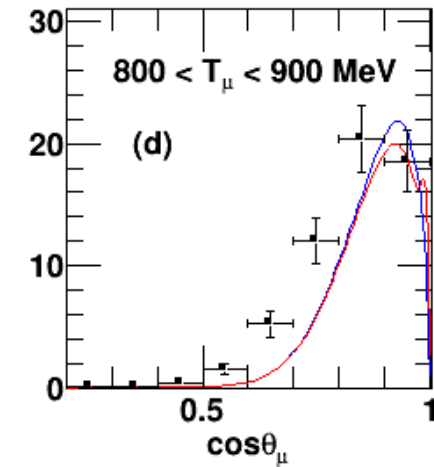
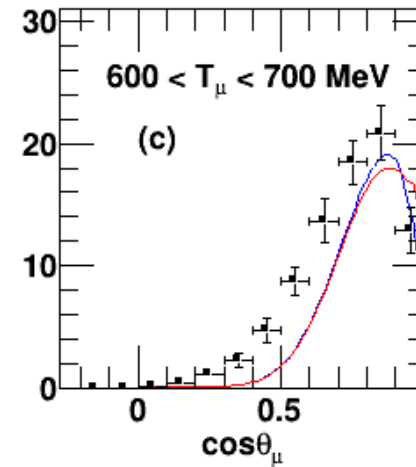
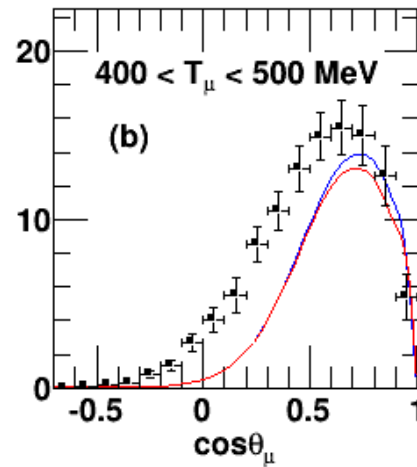
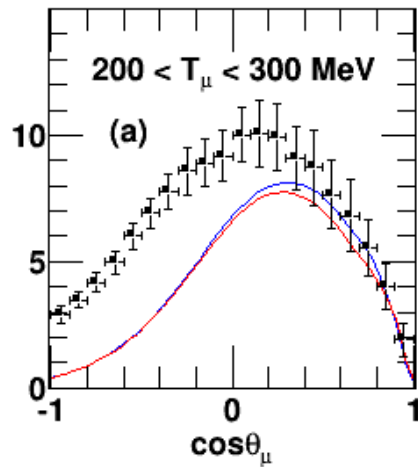


- Good overall agreement with e-scattering data

P. Barreau et al., Nucl. Phys. A402, 515 (1983), J. S. O'Connell et al., Phys. Rev. C35, 1063 (1987), R. M. Sealock et al., Phys. Rev. Lett.62, 1350 (1989), D. S. Bagdasaryan et al., YERPHI-1077-40-88 (1988), D. B. Day et al., Phys. Rev. C 48, 1849 (1993), D. Zeller, DESY-F23-73-2 (1973).

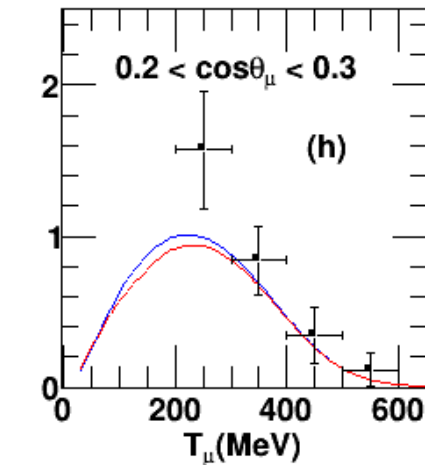
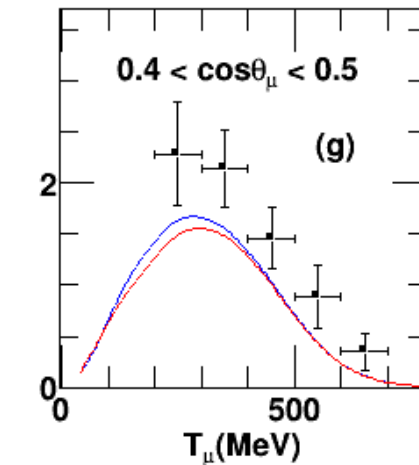
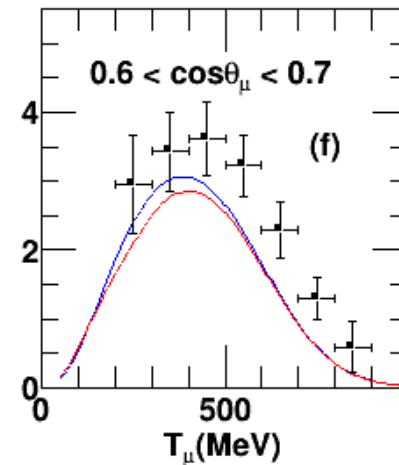
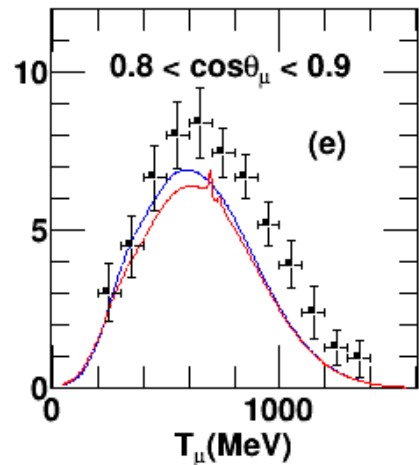
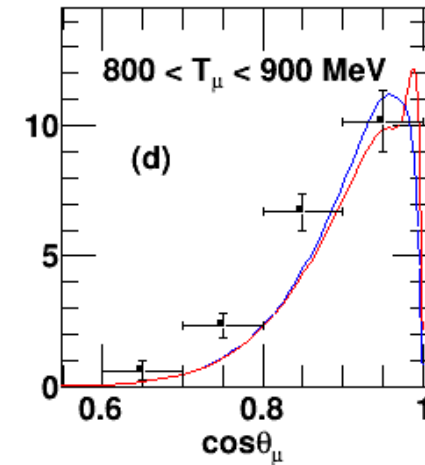
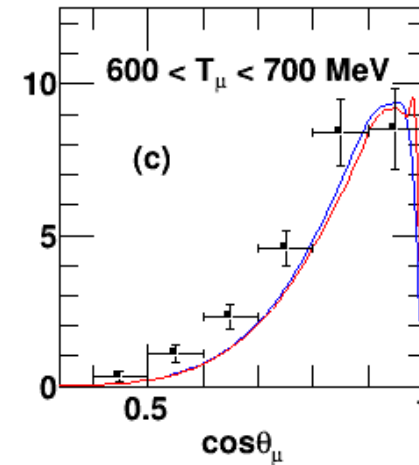
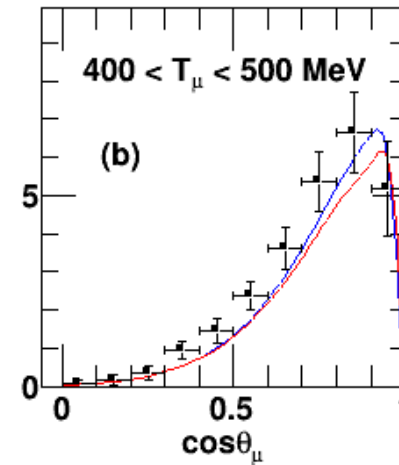
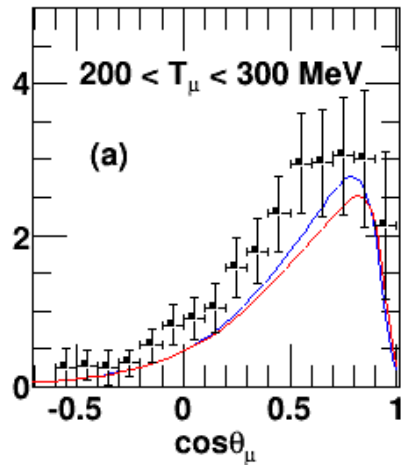
MiniBooNe ν_μ

- Satisfactory general agreement
- Good agreement for forward scattering
- Missing strength for low T_μ , backward scattering



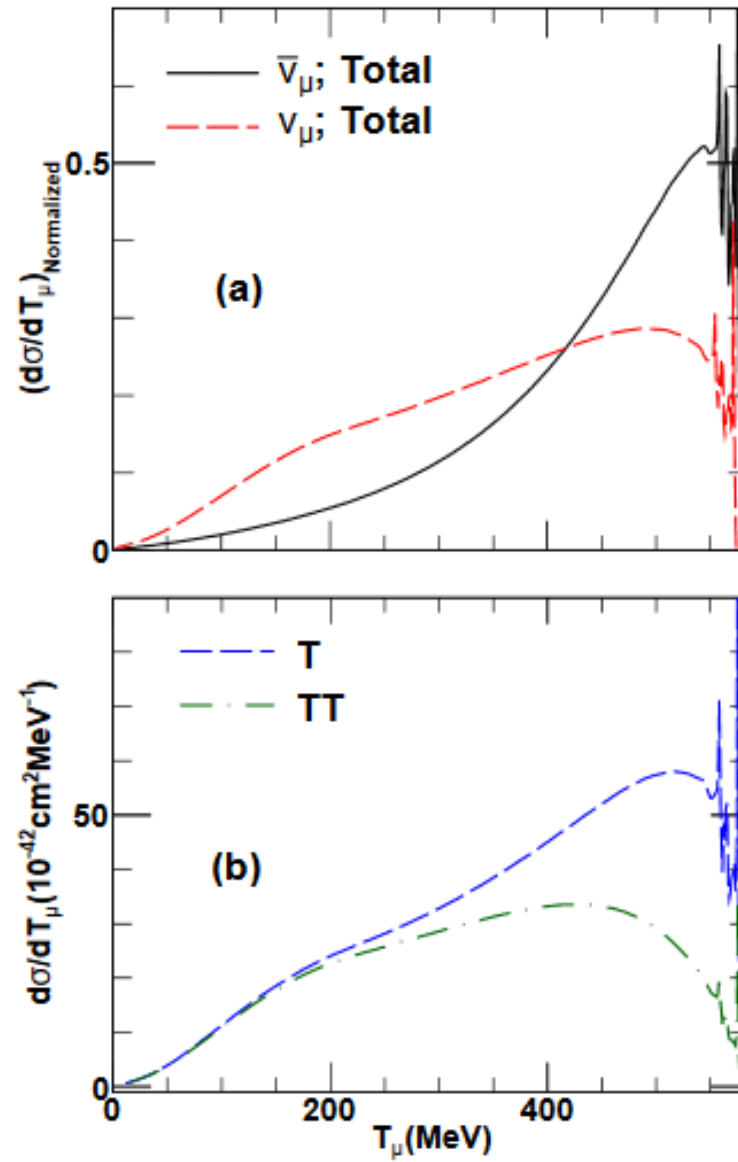
MiniBooNe $\bar{\nu}_\mu$

- Good general agreement
- Good agreement for forward scattering
- Missing strength for high T_μ , backward scattering
- Better agreement with data than neutrino cross sections

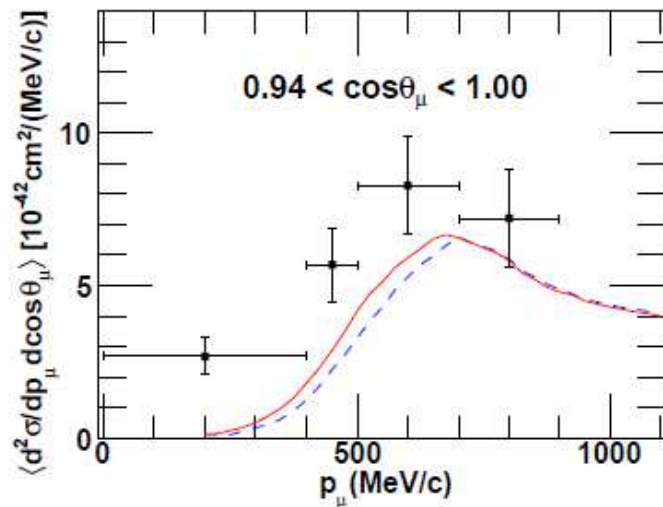
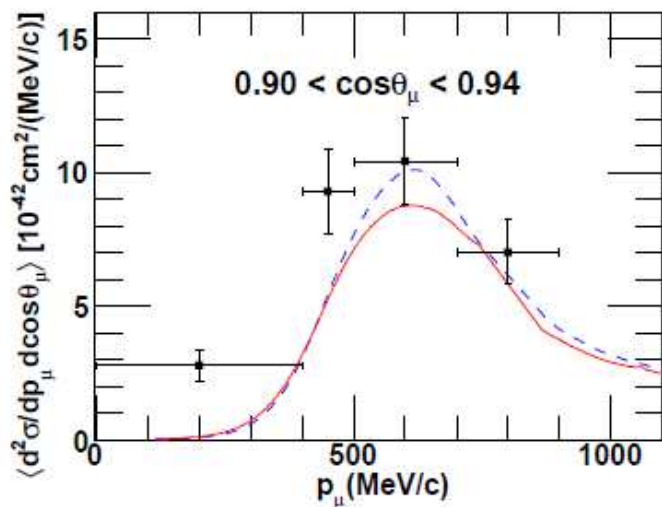
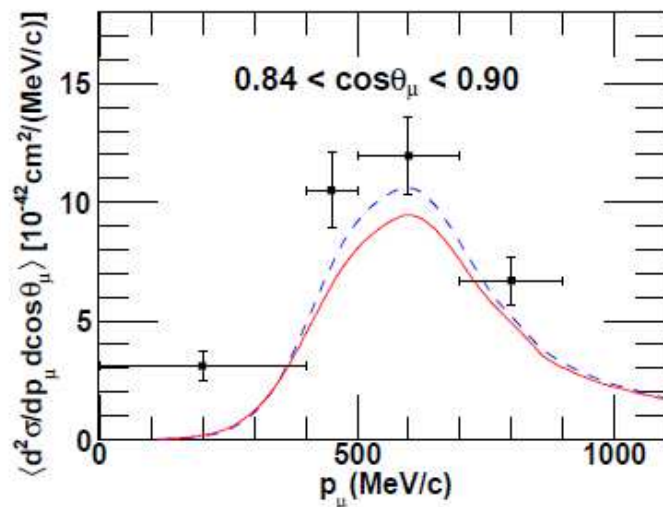
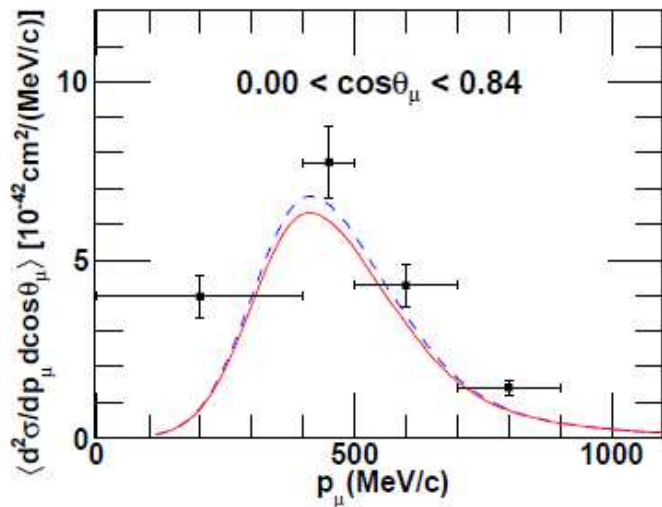


neutrino vs anti
neutrinos

E=700 MeV



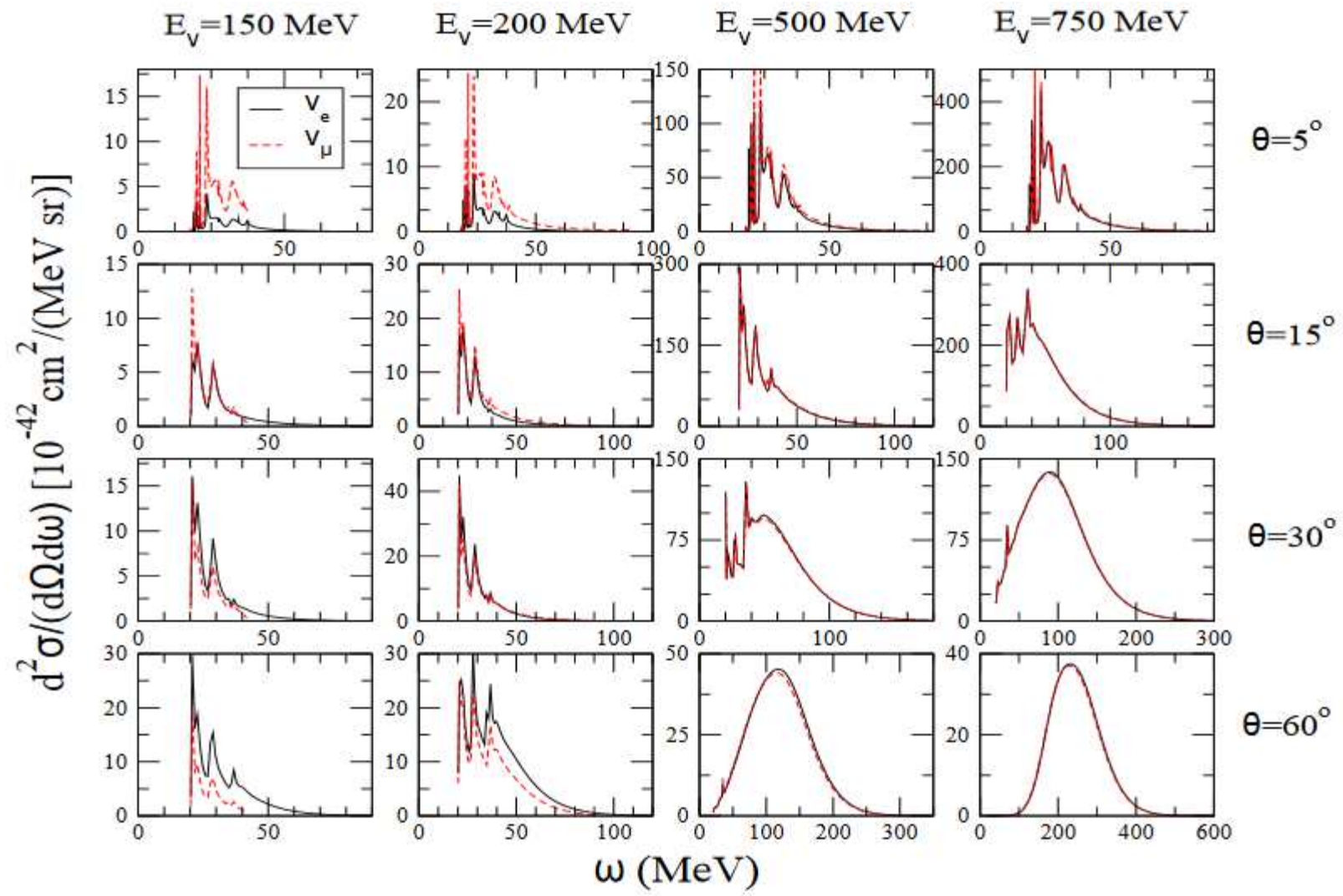
V. Pandey et al, Phys. Rev. C 92, 024606 (2015)



T2K ν_μ

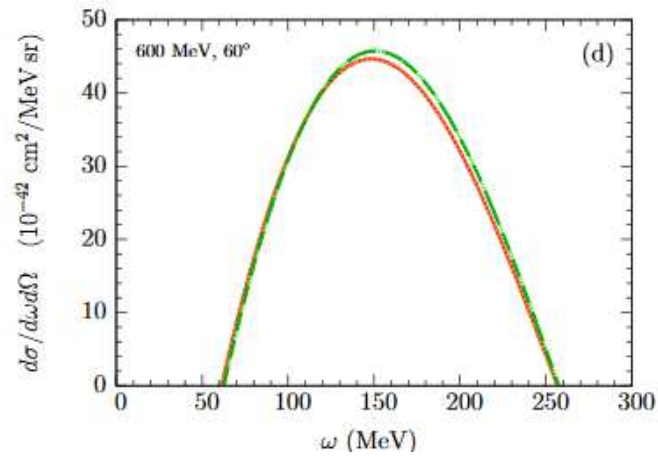
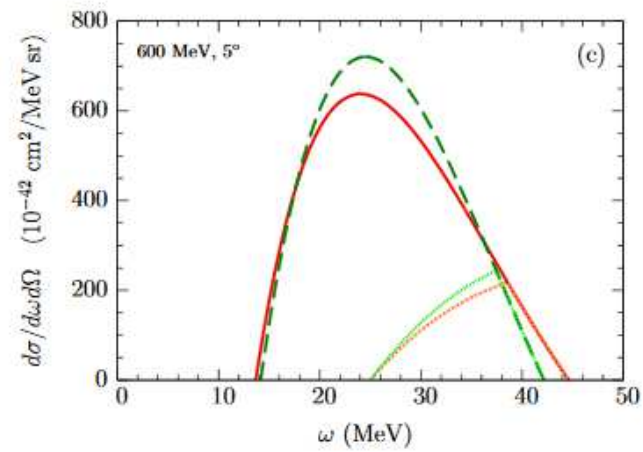
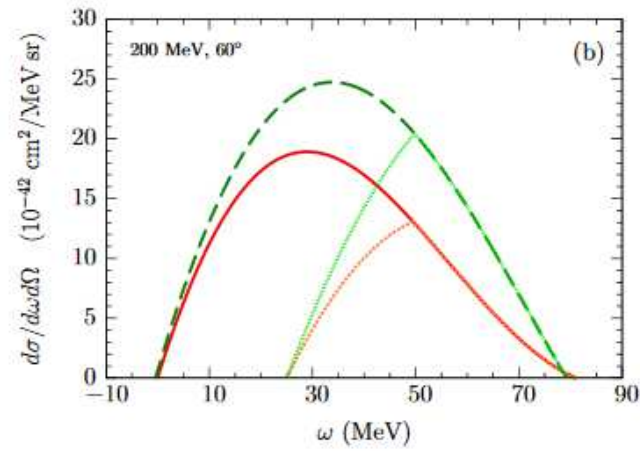
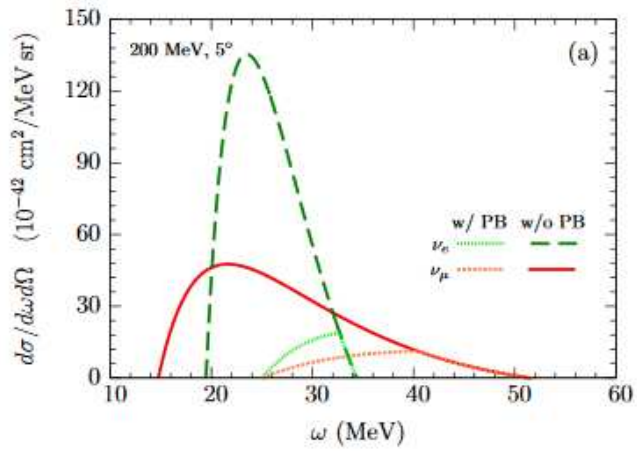
- General agreement quite good
- Missing strength for low p_μ

electron vs muon
neutrinos



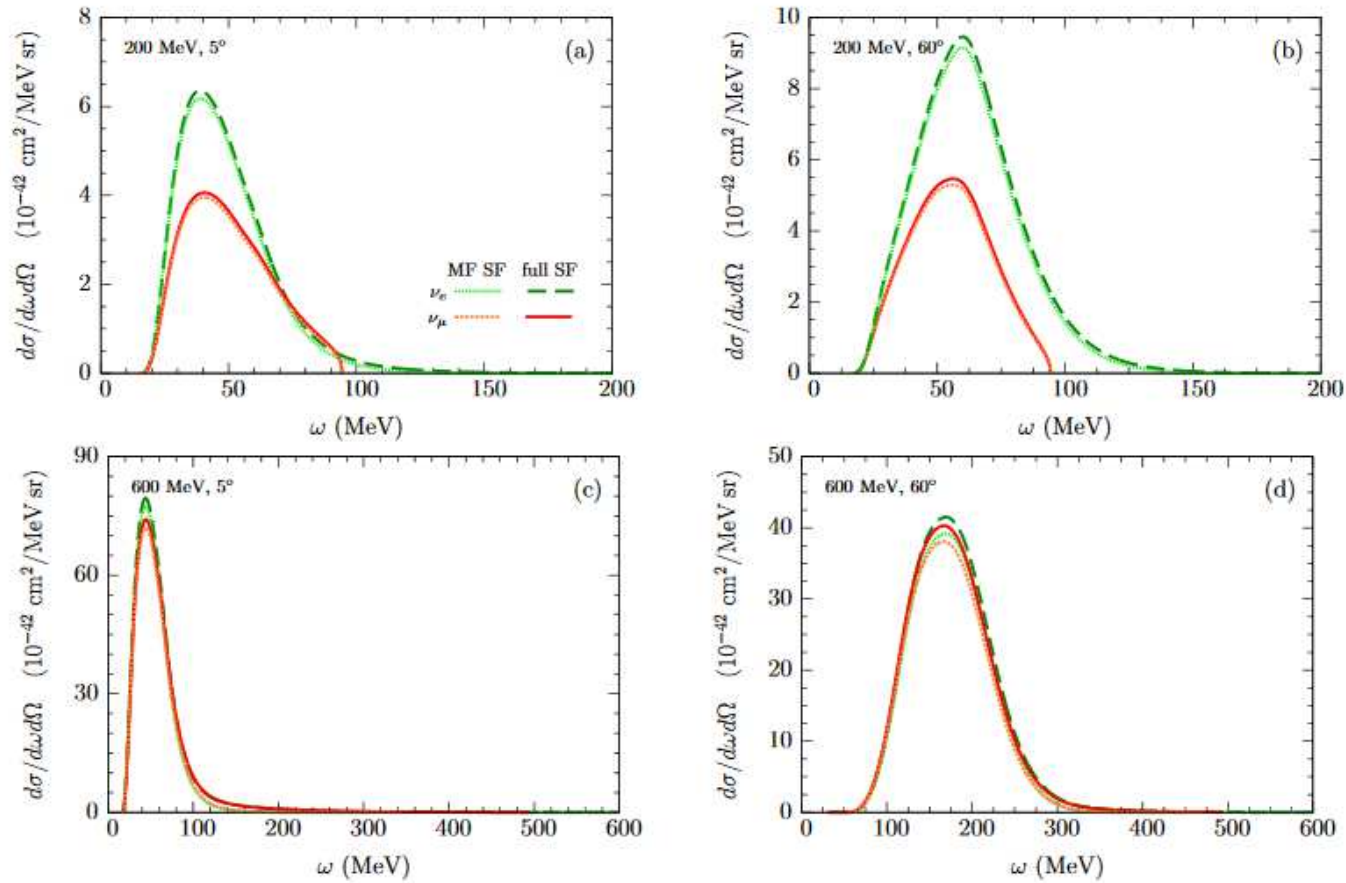
M. Martini et al, Phys.Rev. C94 (2016) no.1, 015501

Fermi gas

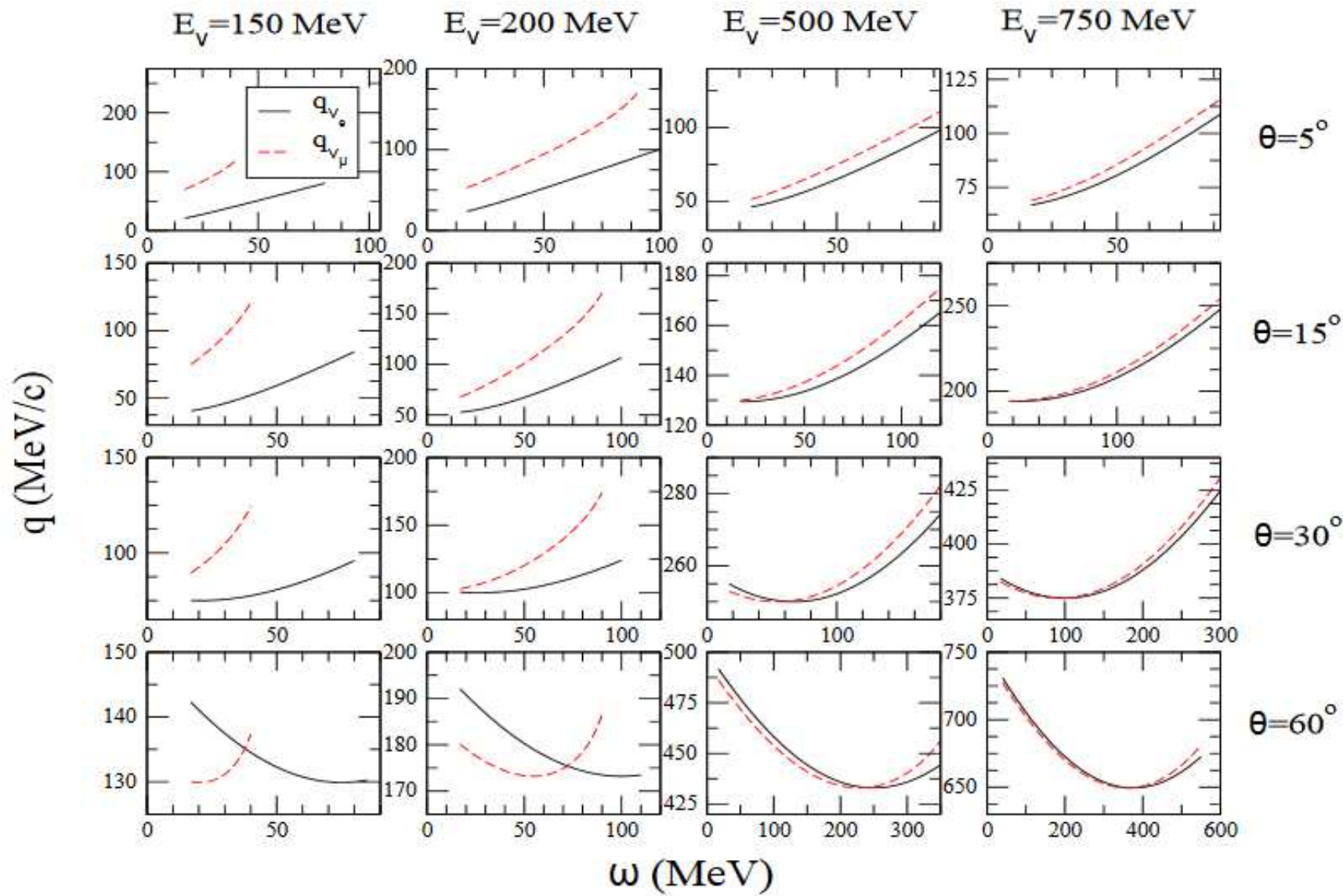


A. Ankowski Phys. Rev. C 96, 035501 (2017)

Spectral function

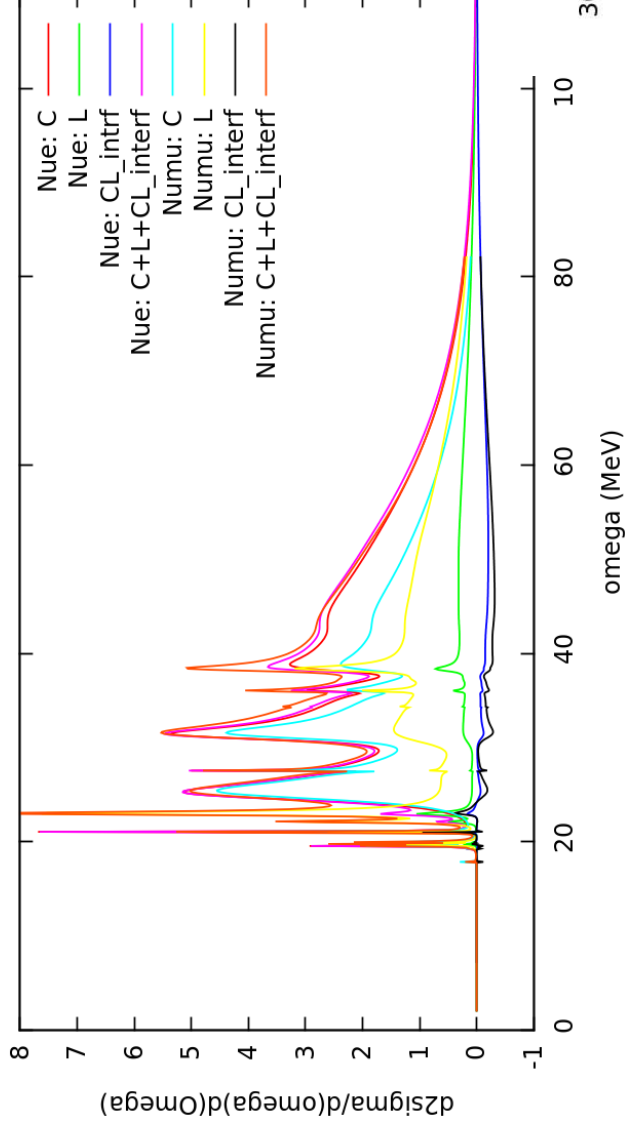


A. Ankowski Phys. Rev. C 96, 035501 (2017)

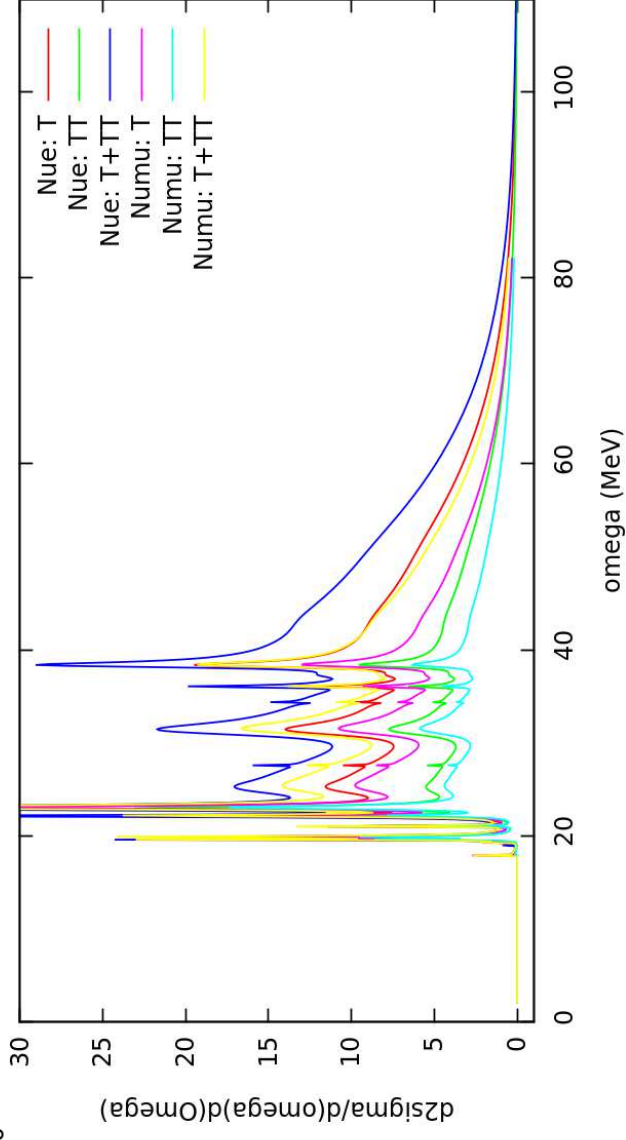


M. Martini et al, Phys.Rev. C94 (2016) no.1, 015501

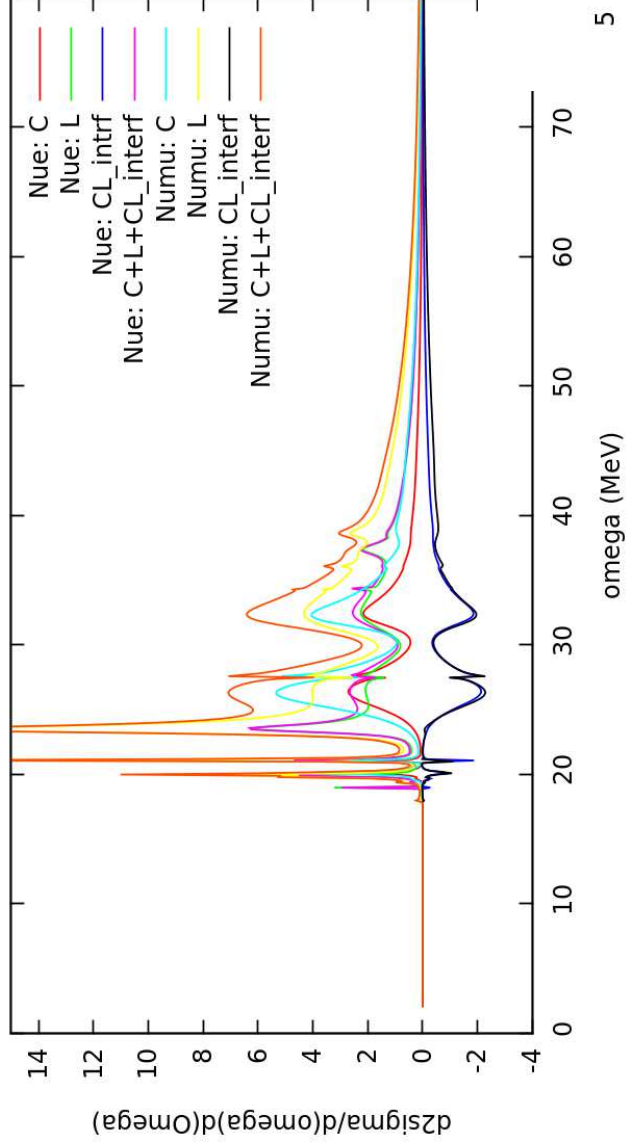
E = 200 MeV, Theta = 60 degrees



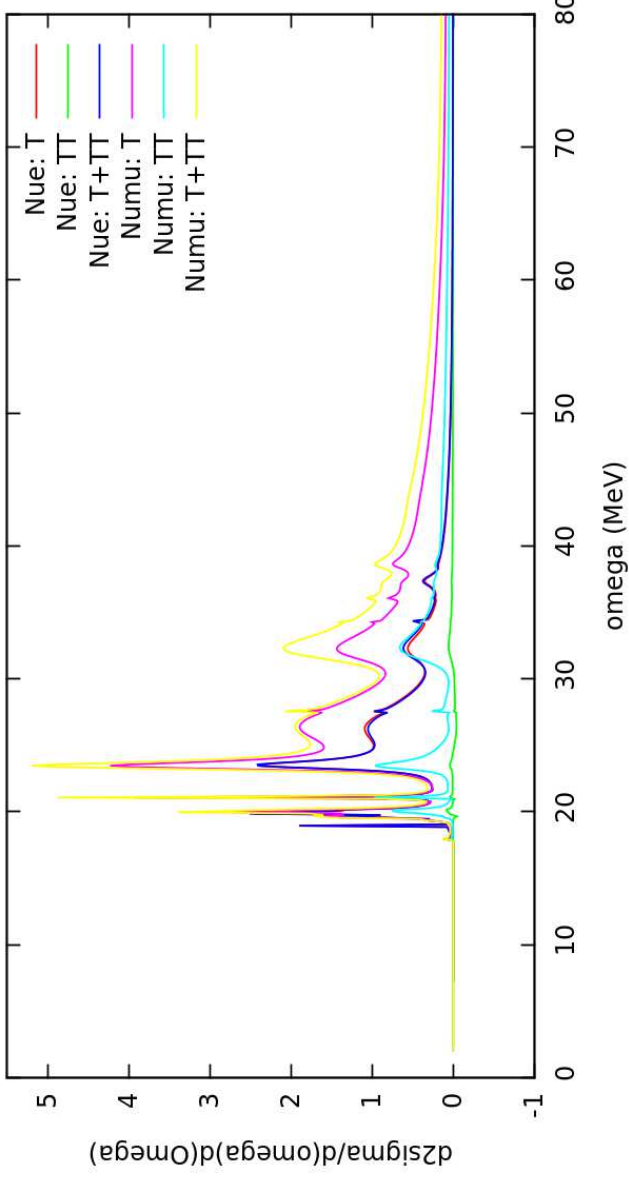
E = 200 MeV, Theta = 60 degrees



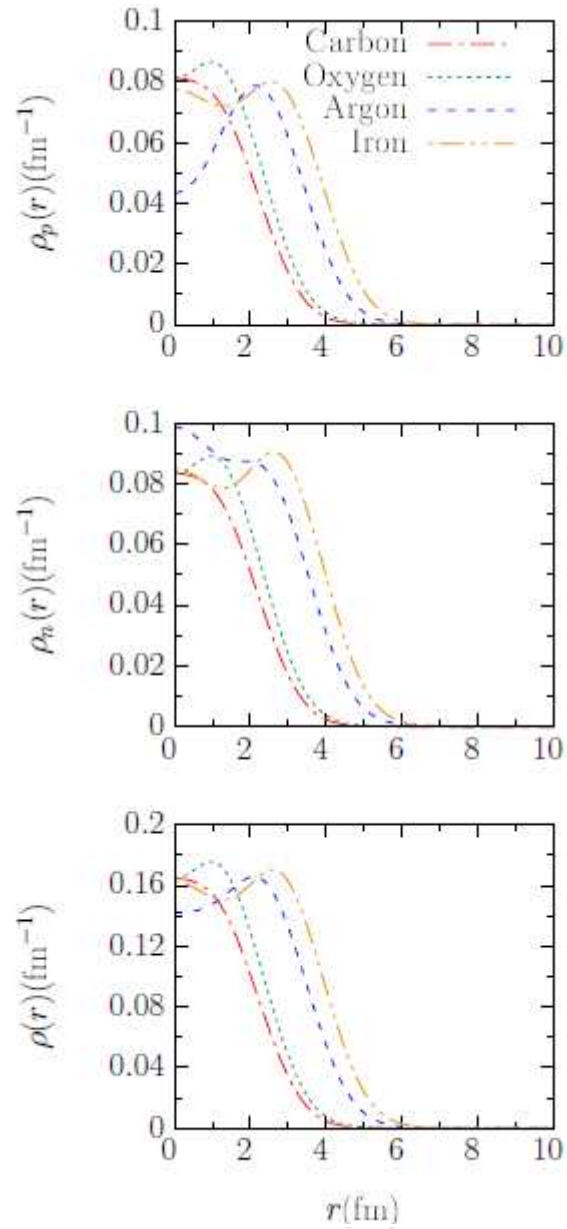
E = 200 MeV, Theta = 5 degrees

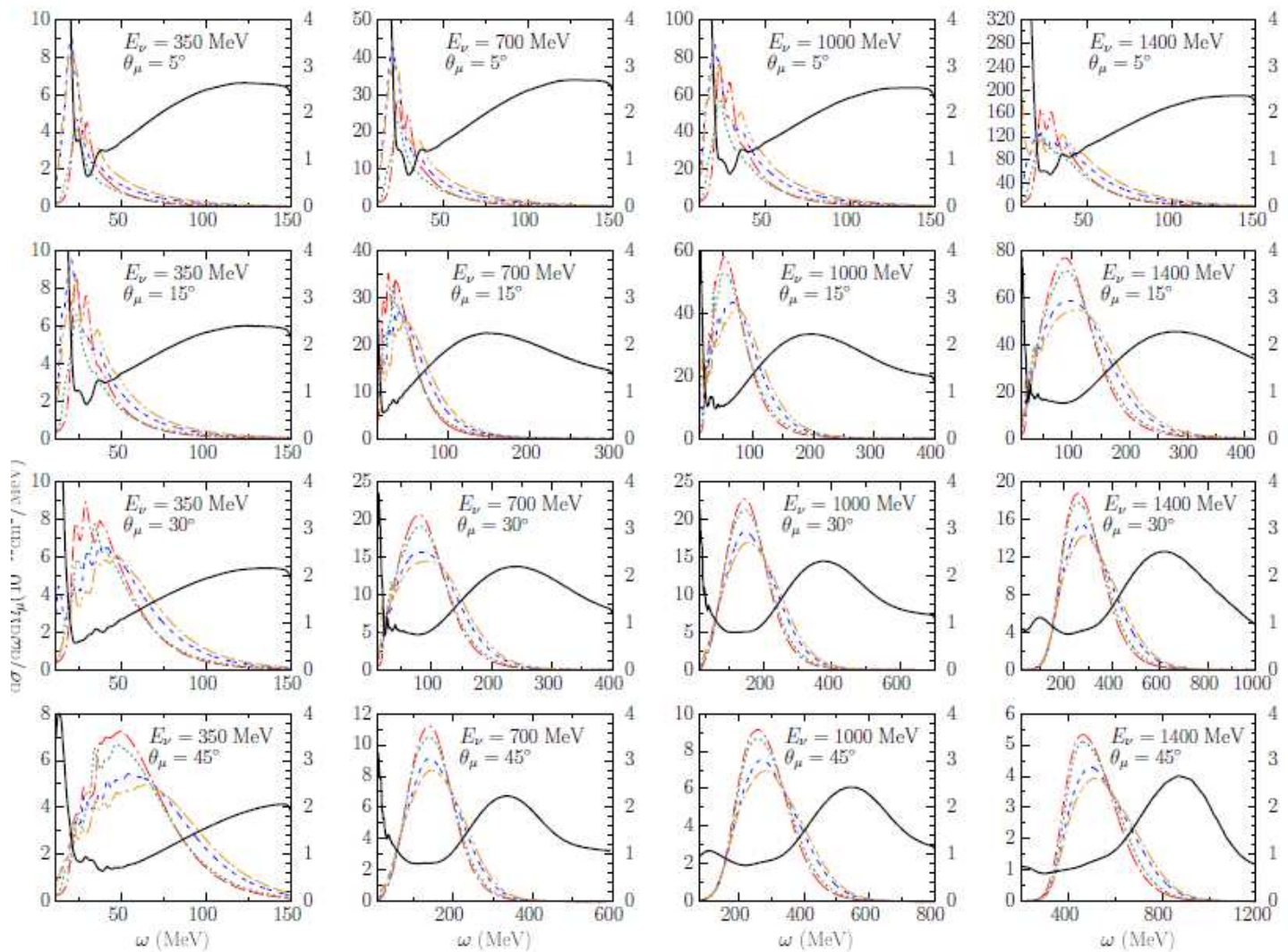


E = 200 MeV, Theta = 5 degrees



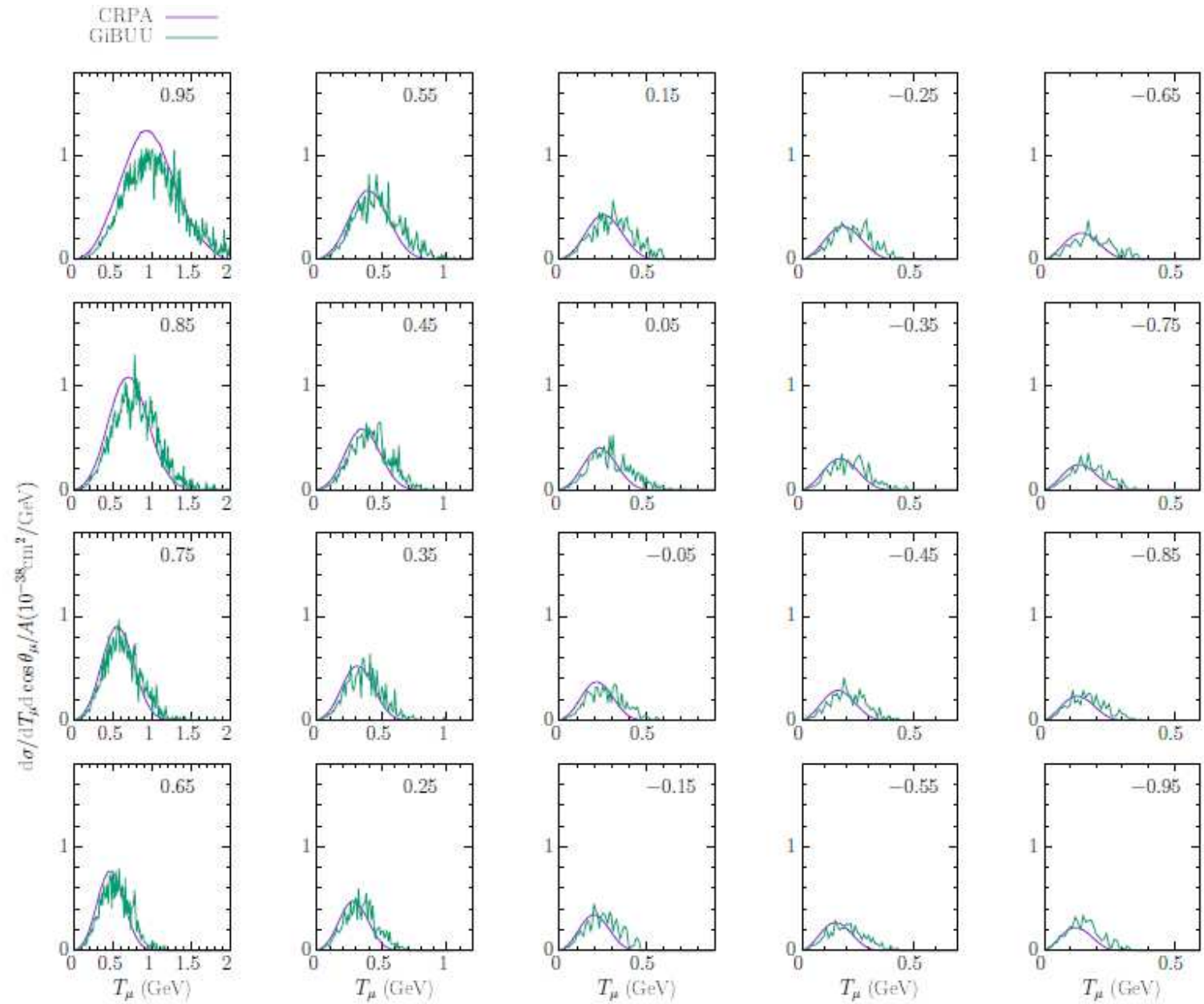
A-dependence of
the cross sections



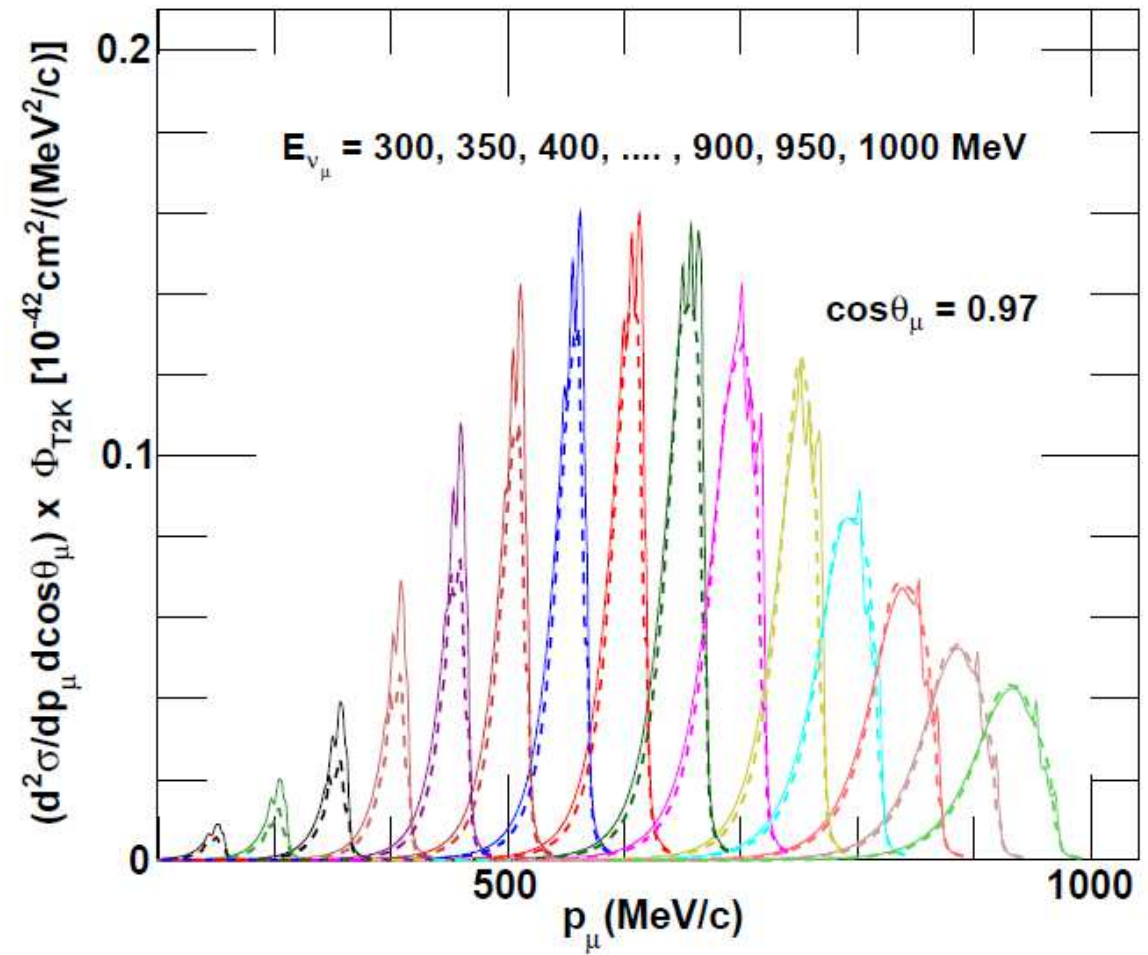


Carbon - - -
 Oxygen - - -
 Argon - - -
 Iron - - -

^{40}Ar

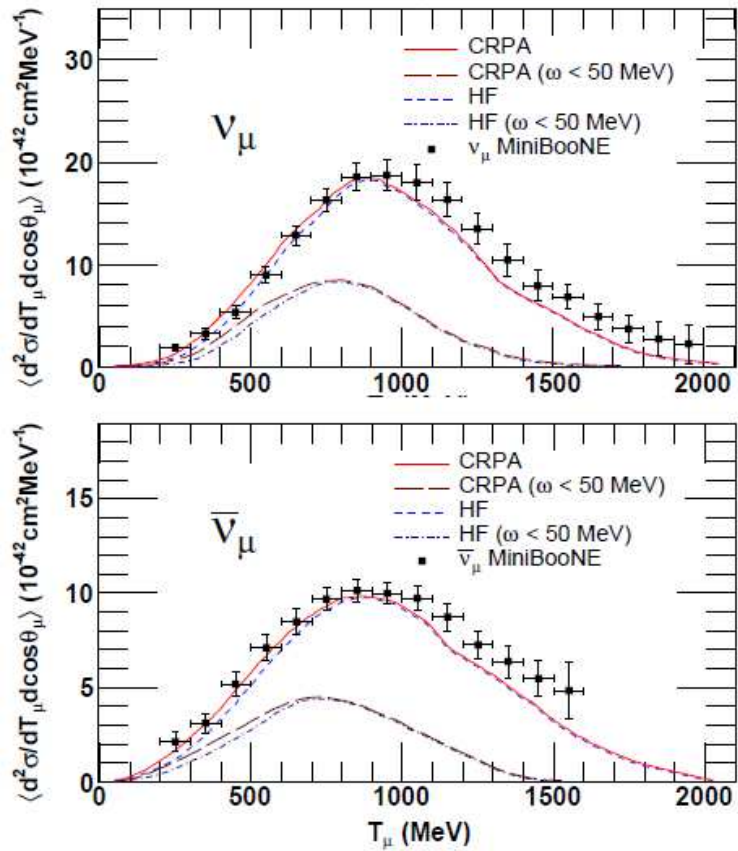


Forward scattering



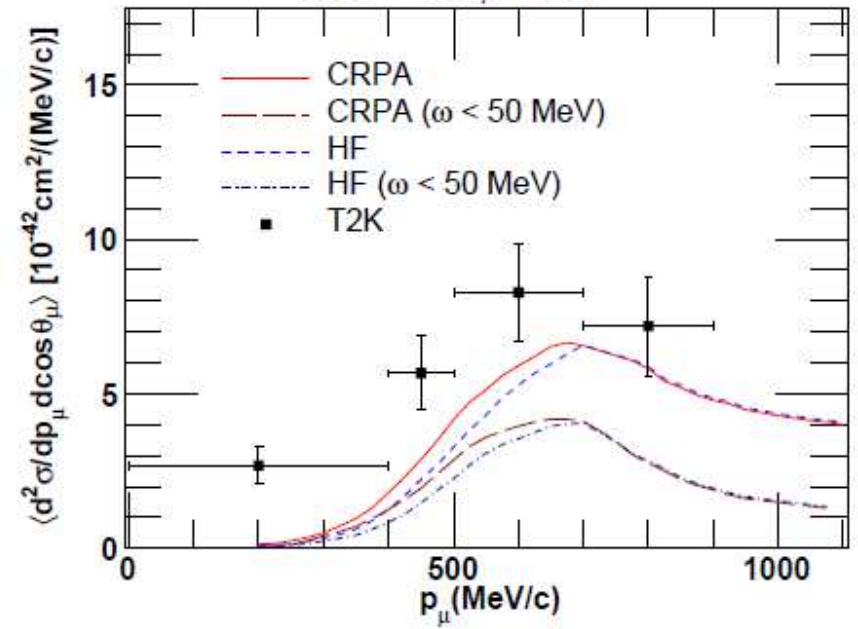
MiniBooNe

$0.9 < \cos\theta_\mu < 1.0$

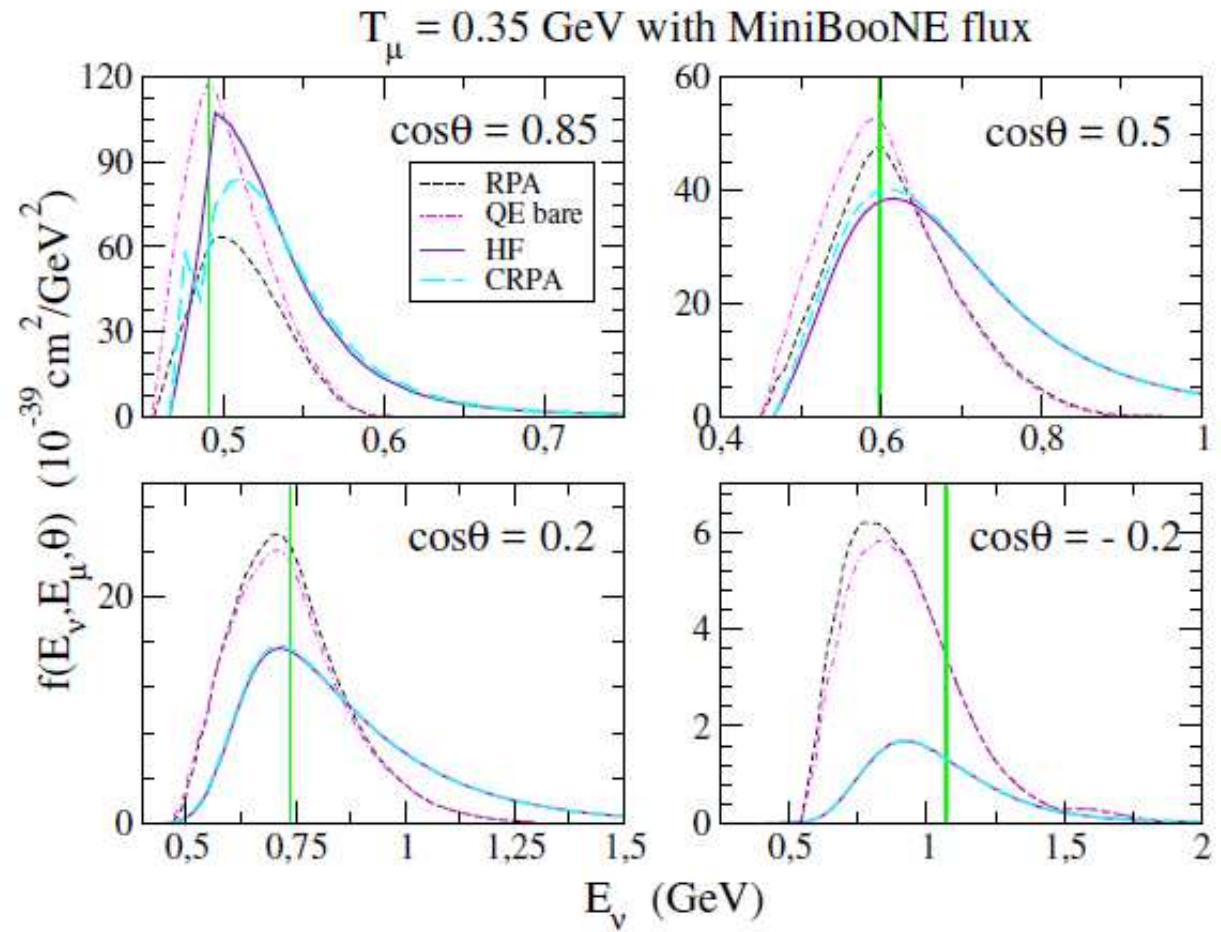


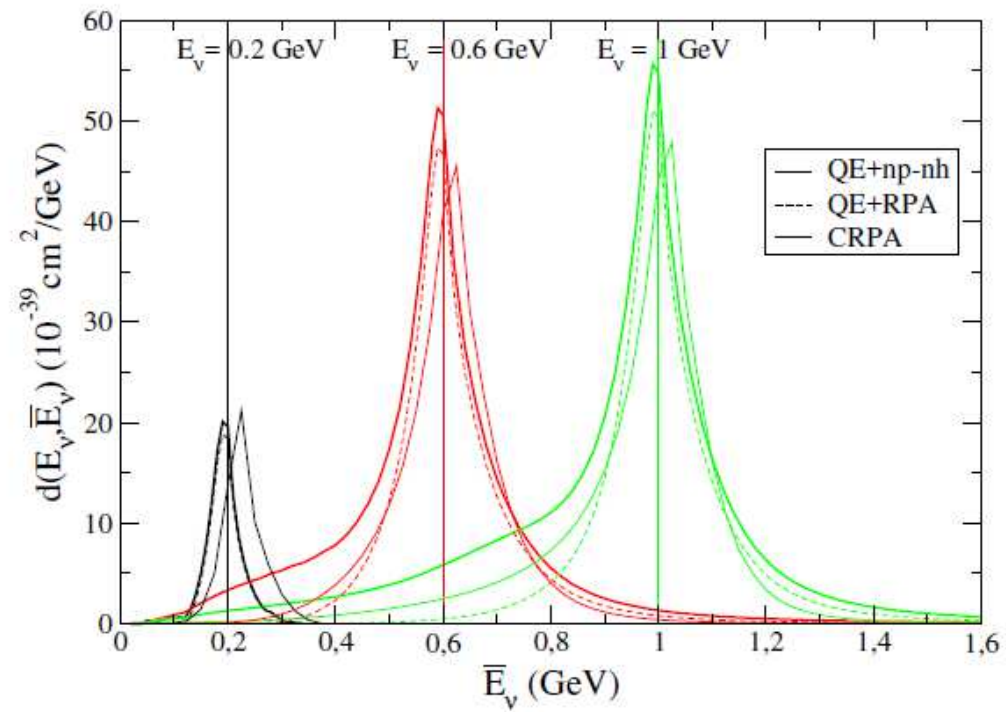
T2K

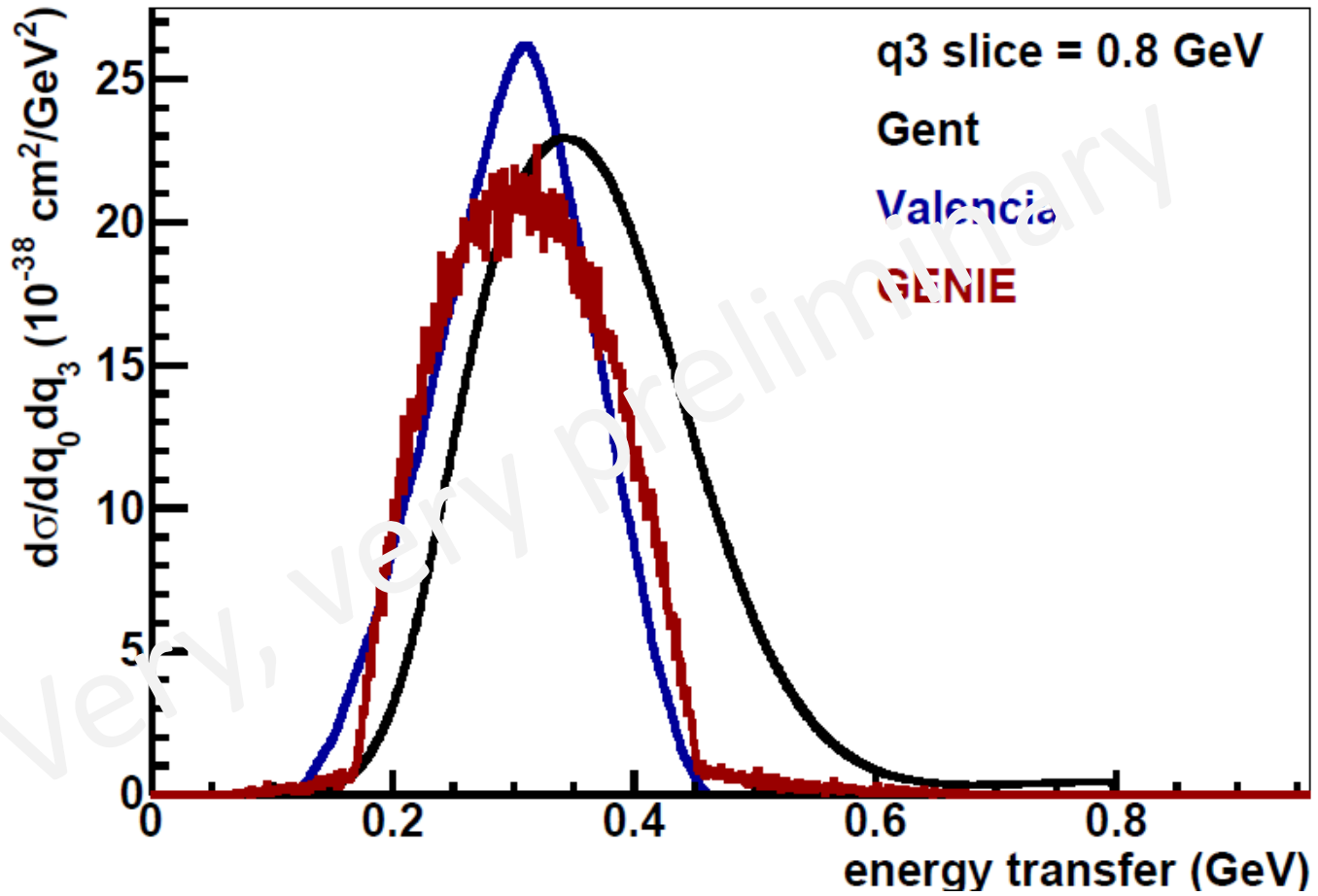
$0.94 < \cos\theta_\mu < 1.00$



Influence of HF-
CRPA on energy
reconstruction



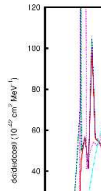




Rik Gran

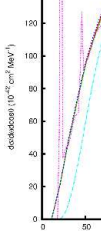
Total

E=500 MeV

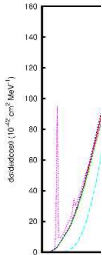


Relativistic corrections

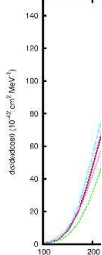
E=750 MeV



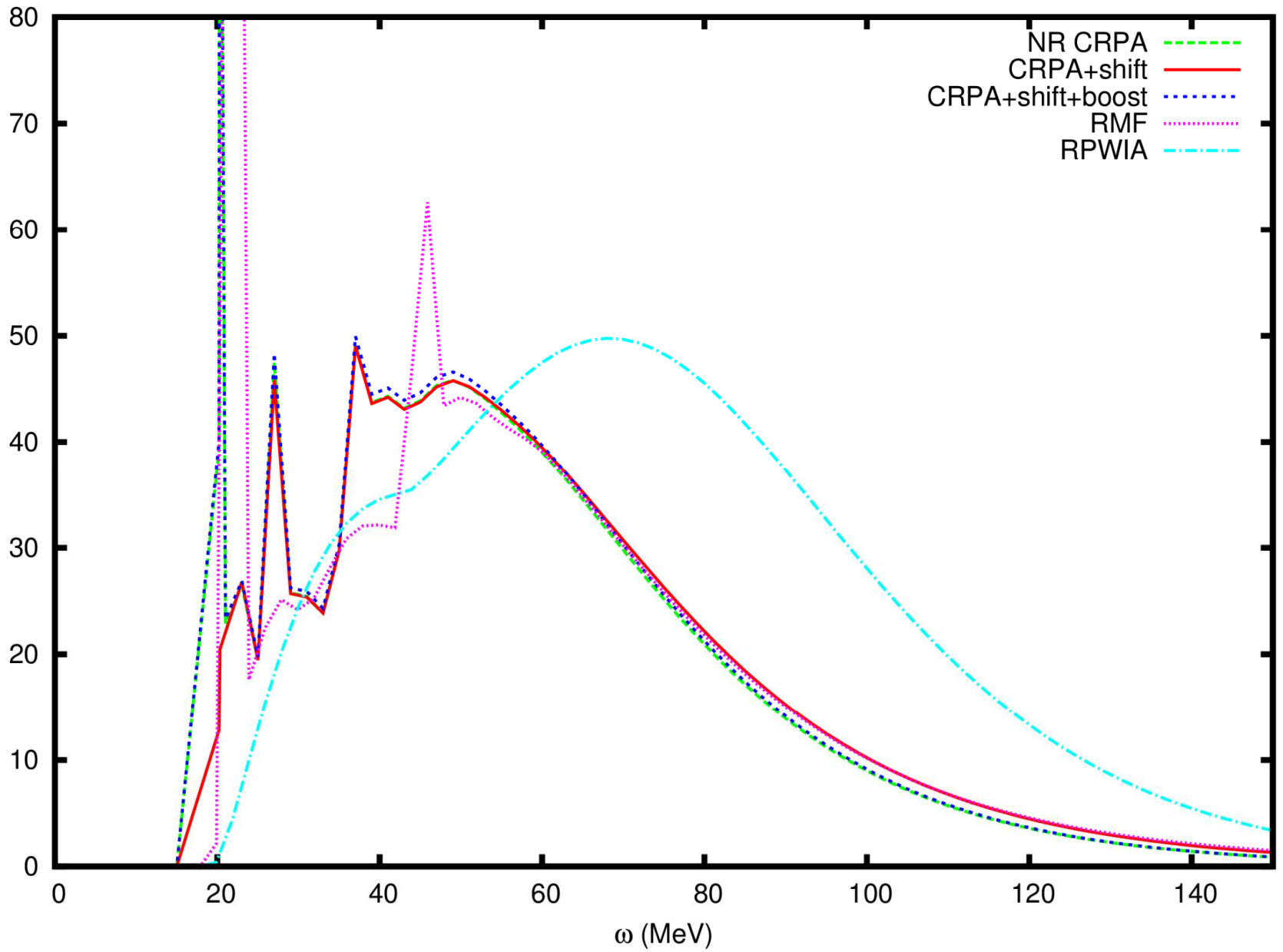
E=1000 MeV



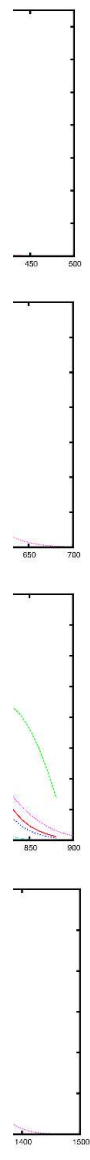
E=1500 MeV



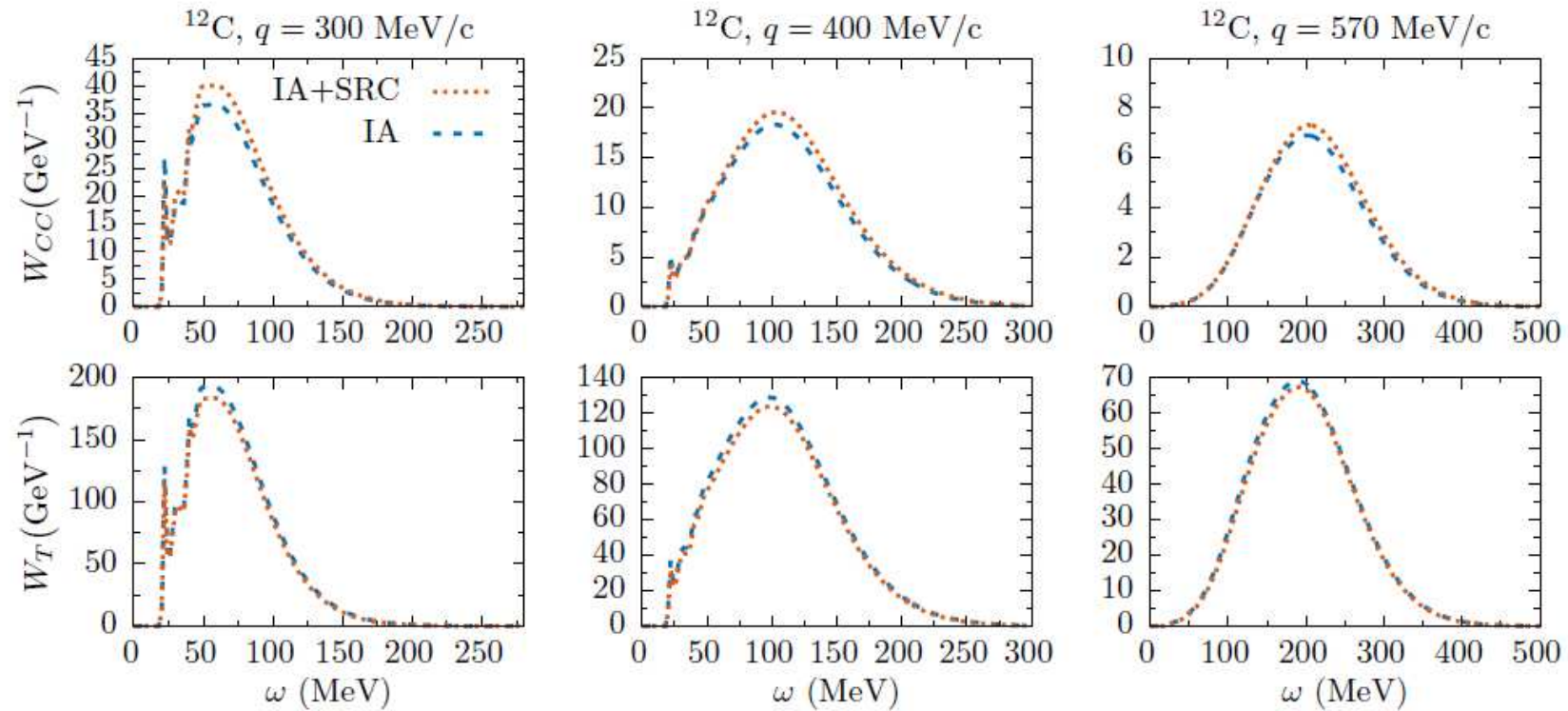
$d\sigma/d\omega d\cos\theta$ ($10^{-42} \text{ cm}^2 \text{ MeV}^{-1}$)



NR CRPA
CRPA+shift
CRPA+shift+boost
RMF
RPWIA



SRC neutrinos 1p1h

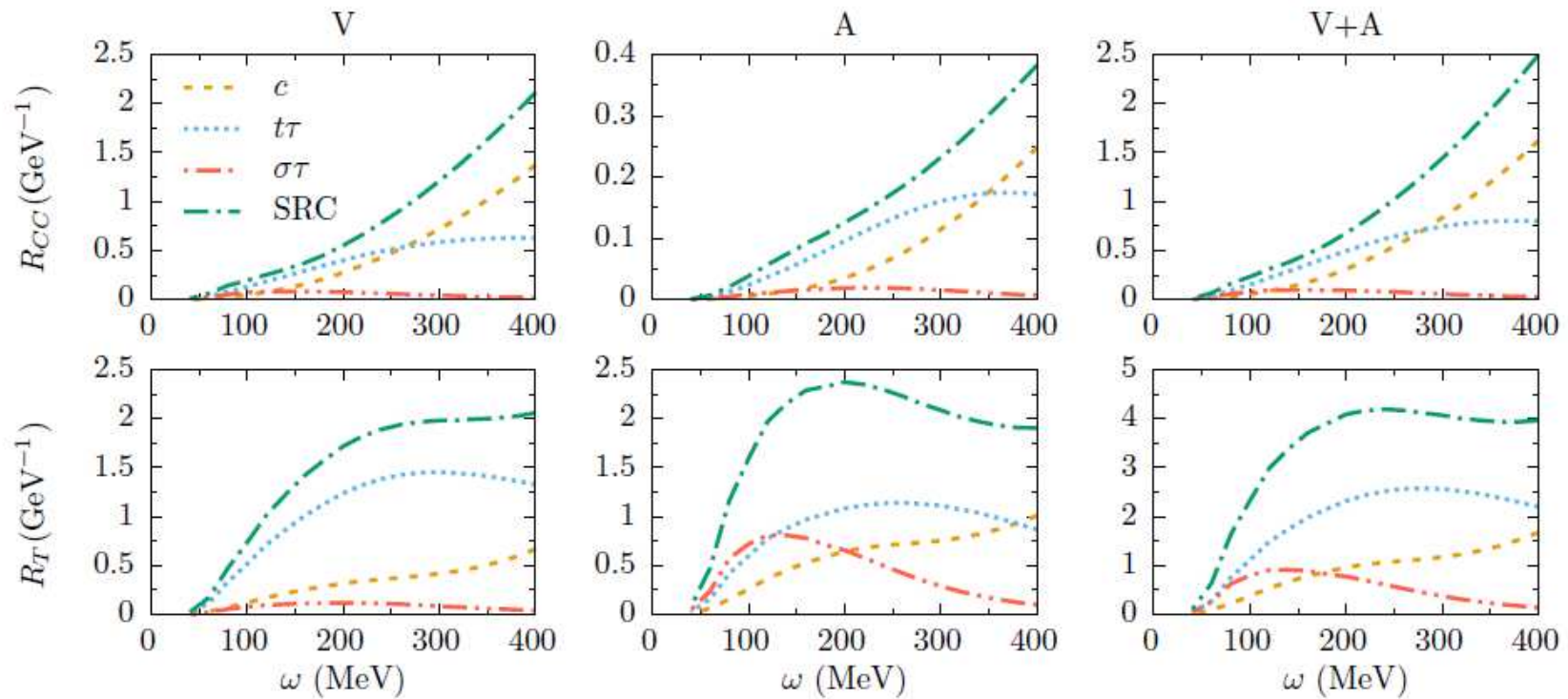


- Reduction of transverse response
- Enhancement of Coulomb-longitudinal

T. Van Cuyck, N. Jachowicz, R. González-Jiménez, *et al.* [Phys. Rev. C94, 024611 \(2016\)](#).

SRC neutrinos 2p2h

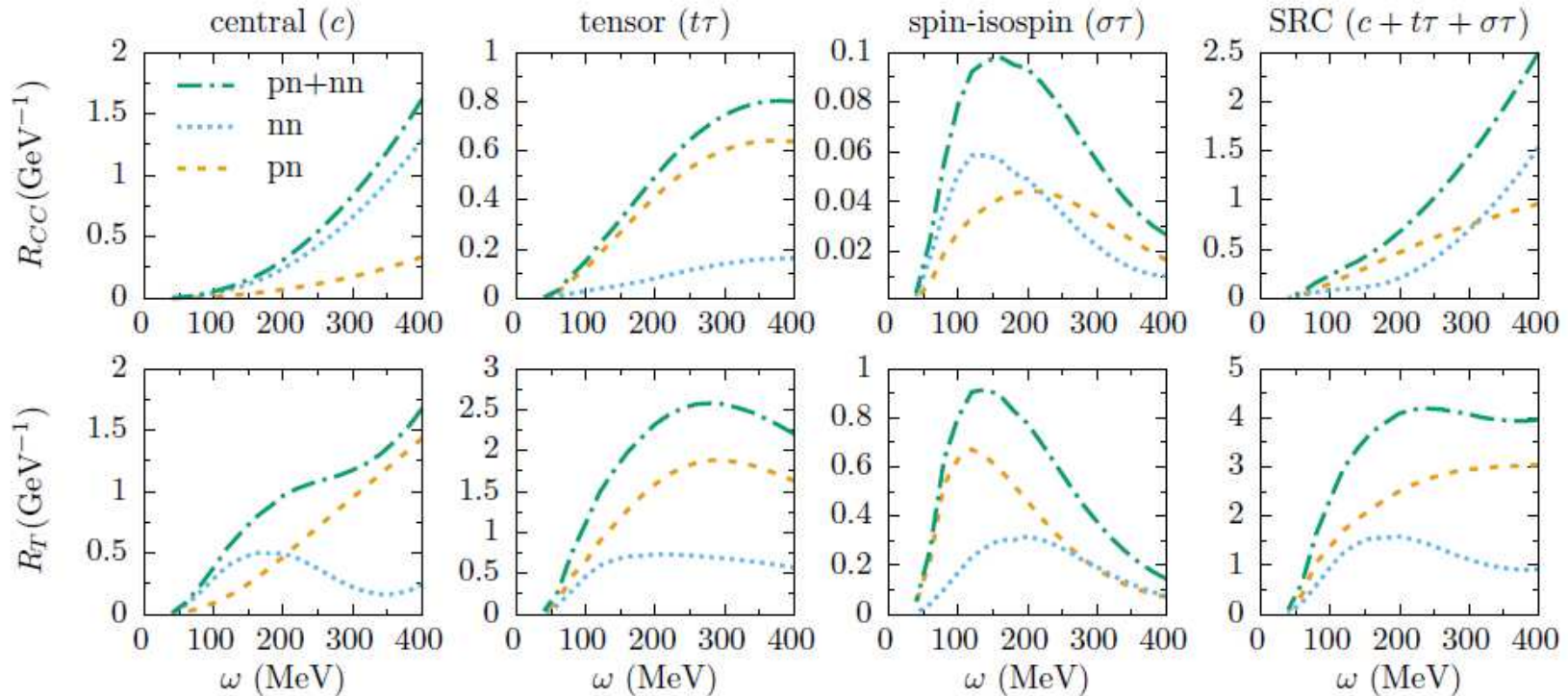
$q = 400 \text{ MeV}/c$



- Vector and axial contributions have comparable strength
- Tensor often dominates, but not for all kinematics

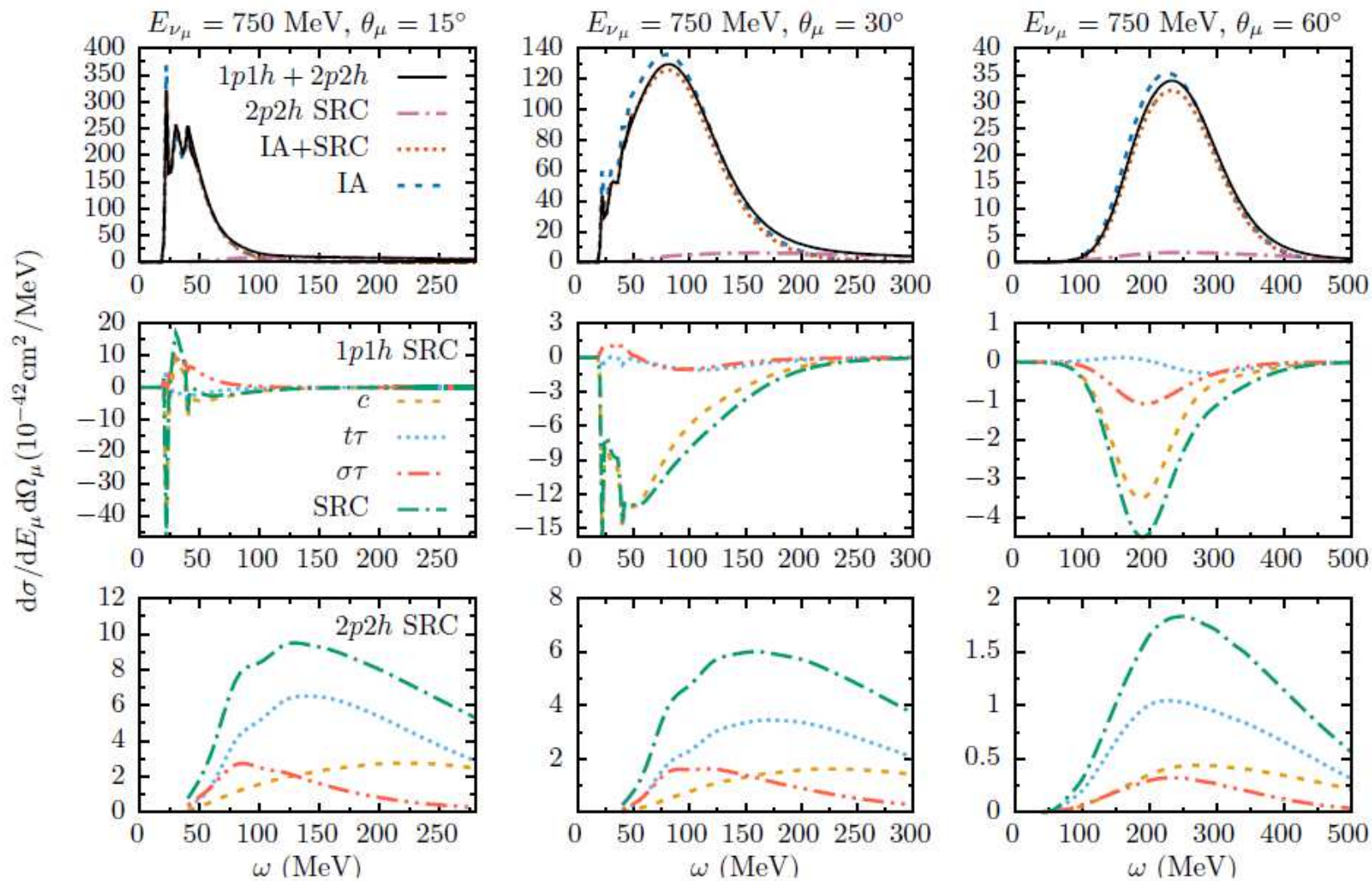
SRC neutrinos 2p2h

$q = 400 \text{ MeV}/c$.



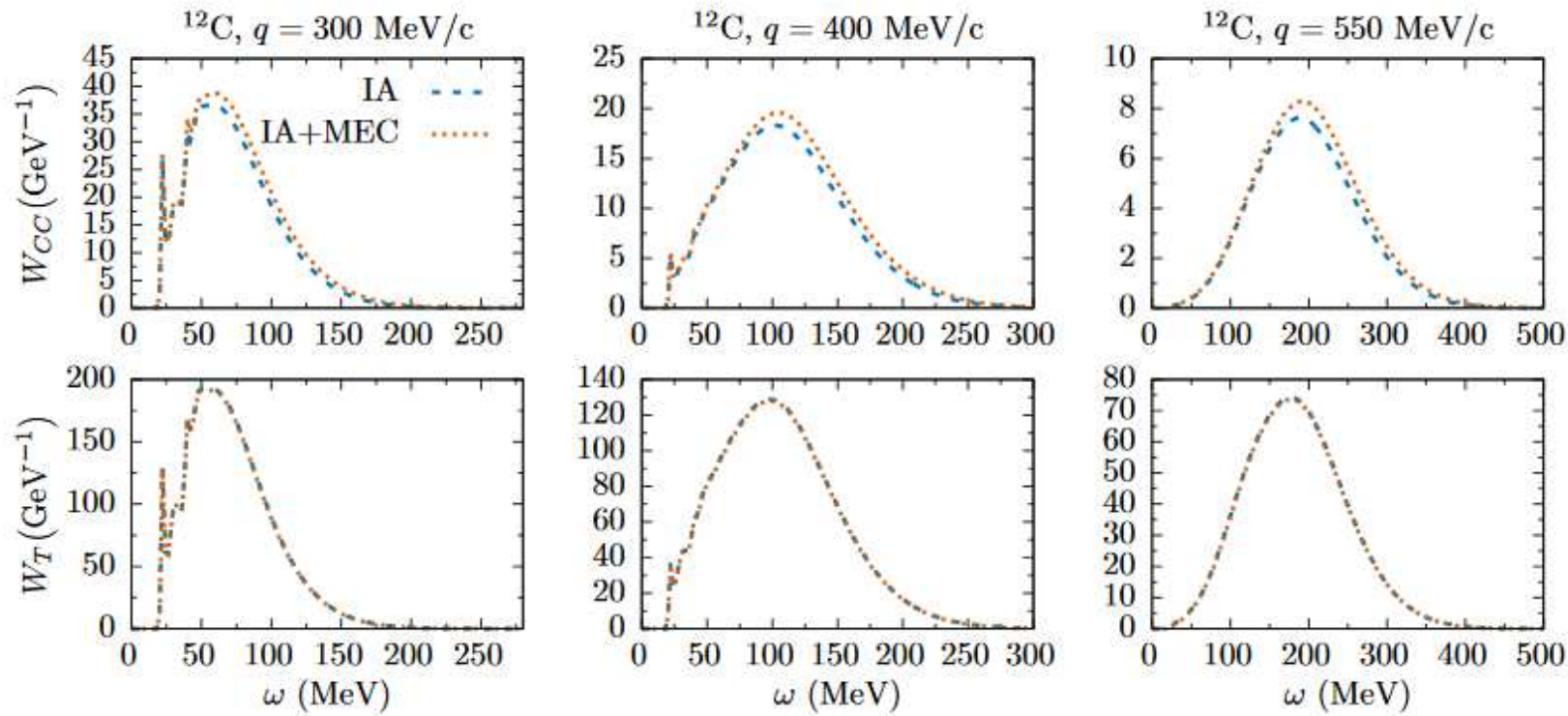
- Vector and axial contributions have comparable strength
- Tensor often dominates, but not for all kinematics
- pn pairs dominate

SRC neutrinos 1p1h+2p2h



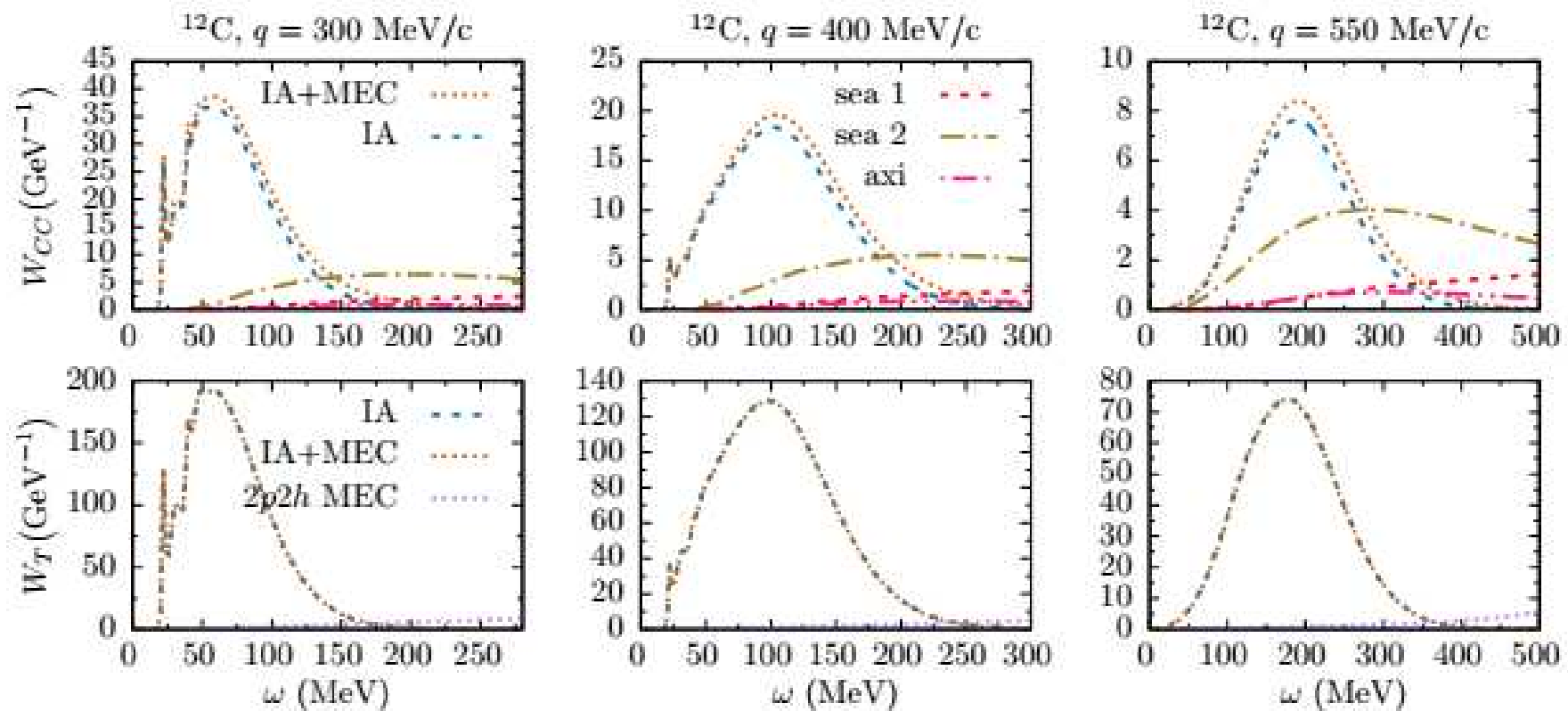
T. Van Cuyck et al
Phys. Rev. C 94,
024611 (2016)

Seagull and PIF in neutrino 1p1h

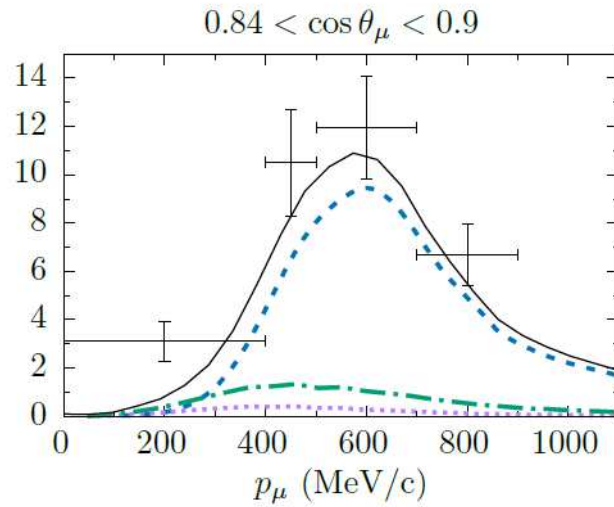
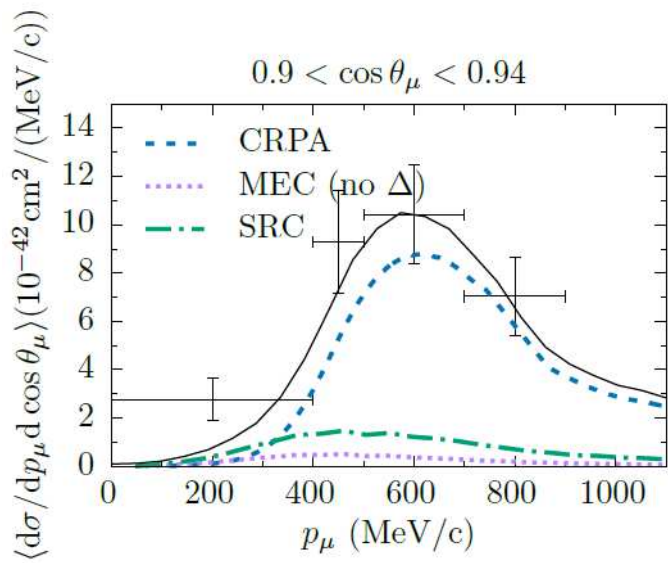


T. Van Cuyck, N. Jachowicz, R. González-Jiménez, *et al* PRC95, 054611 (2017)

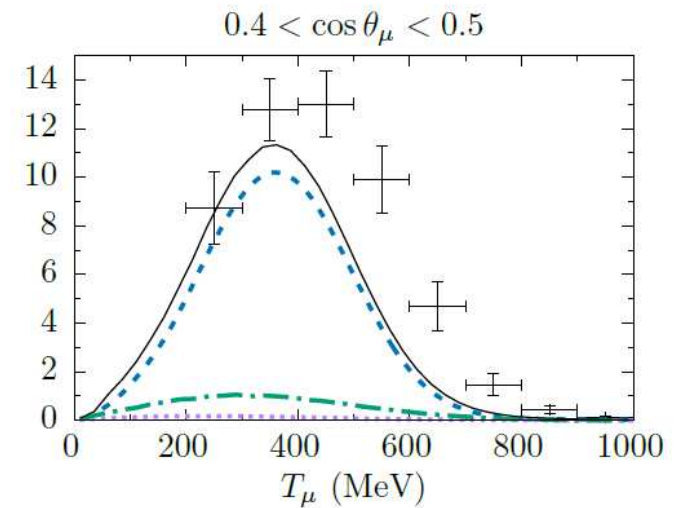
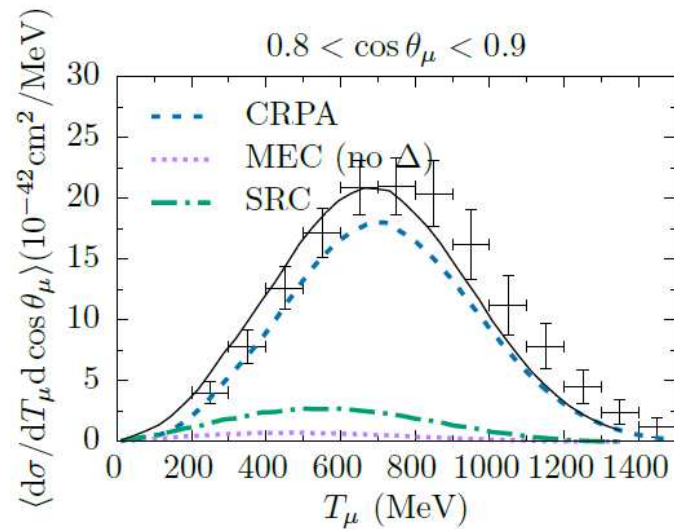
Seagull and PIF in neutrino 2p2h



T2K



MiniBooNe



Summary

- Long- and short-range correlations in QE-like cross sections
- CRPA calculations provide extra strength for forward scattering arising from low-energy excitations
- This might affect CCQE neutrino cross sections as measured by MiniBooNe, T2K, ...
- SRC and MEC affect 1- and 2-nucleon knockout processes